Louisiana State University
LSU Digital Commons

LSU Master's Theses | Graduate School

2008

Adjustable speed drives laboratory based on dSPACE controller

Kiran Kumar Gunda
Louisiana State University and Agricultural and Mechanical College, kgunda1@lsu.edu

Follow this and additional works at: https://digitalcommons.lsu.edu/gradschool_theses

Part of the Electrical and Computer Engineering Commons

Recommended Citation
Gunda, Kiran Kumar, "Adjustable speed drives laboratory based on dSPACE controller" (2008). *LSU Master's Theses*. 2301.
https://digitalcommons.lsu.edu/gradschool_theses/2301

This Thesis is brought to you for free and open access by the Graduate School at LSU Digital Commons. It has been accepted for inclusion in LSU Master's Theses by an authorized graduate school editor of LSU Digital Commons. For more information, please contact gradetd@lsu.edu.

ADJUSTABLE SPEED DRIVES LABORATORY BASED ON DSPACE CONTROLLER

A Thesis
Submitted to the Graduate Faculty of the
Louisiana State University and
Agricultural and Mechanical College
in partial fulfillment of the
requirements for the degree of
Master of Science in Electrical Engineering

in

The Department of Electrical & Computer Engineering

by
Kiran Kumar Gunda
Bachelor of Technology, Jawaharlal Nehru Technological University, 2005
August 2008

Dedicated to my dearest parents

and

Tom

Acknowledgements

I would like to express my gratitude to my advisor, Dr. Ernest A. Mendrela for his constant encouragement and guidance throughout the research. His technical advice and expertise in the field helped me to cross all the hurdles towards the successful completion of this thesis. I would also like to thank him for being patience with me during my thesis and write up.

I would like to thank my committee members Dr. Martin Feldman and Dr. Hsiao-Chun Wu for sparing time out of their busy schedule and agreeing to be a part of my committee. I would like to thank Thomas N. Walsh for supporting me during my stay at LSU and providing me lot of courage and encouragement to achieve success in my thesis and in my real life.

I can't express myself how thankful I am to my parents for their support and love provided by them throughout my life. I would like to thank my dearest cousin Sudheer Pinna and my sister-in-law Hymavathi Pinna for their constant encouragement and continuing advice.

I owe a lot to my roommates Ashok and Ramana for their support in finishing my most prestigious thesis and I would also like to thank all my friends at LSU who made my stay at LSU pleasant and enjoyable.

Table of Contents

Acknowledgements ..... **iii**

List of Tables ..... **vii**

List of Figures ..... **viii**

Abstract ..... **xiii**

Chapter 1. Introduction **1**
1.1 Overview of the Thesis 1
1.2 Objectives of the Thesis 5
1.3 Outline of the Thesis 6

Chapter 2. Experiment 1 – Building a Simple Dynamic Model in Simulink **7**
2.1 Introduction 7
2.2 Theoretical Background 7
2.3 Modeling a Mechanical System in Simulink 8
2.3.1 Simulink Model with Inertia Only 8
2.3.2 Mechanical Model with Friction 10
2.3.3 Mechanical System with Modified Load 11
2.4 Conclusion 14

Chapter 3. Experiment 2 – Building a Simple Real-Time Model in Simulink **15**
3.1 Introduction 15
3.2 Model Description 15
3.3 Simulation in Simulink 16
3.4 Real-Time Modeling Using dSPACE 17
3.5 Conclusion 21

Chapter 4. Experiment 3 – Switch-Mode DC Converter and No-Load DC Motor Test **22**
4.1 Introduction 22
4.2 Theoretical Background 22
4.2.1 Pulse Width Modulation (PWM) of Switching Power Pole 23
4.2.2 Duty Ratio and Switching Function of Single-Pole Converter 24
4.2.3 Two-Pole Converter Model 24
4.3 Simulation of Switch-Mode Converter in Simulink 25
4.3.1 Simulink Model for Single-Pole Converter 25
4.3.2 Simulink Model for Two-Pole Converter 27
4.3.3 Implementation of Two-Pole Converter Model in Real-Time 27
4.4 Speed Control of DC Motor in Open-Loop 30
4.4.1 Real-Time Simulink Model for No-Load DC Motor Test 30
4.5 Results of No-Load DC Motor Test 32

4.6 Conclusion 34

Chapter 5. Experiment 4 – Determination of DC Motor Parameters 35
5.1 Introduction 35
5.2 Steady-State Characteristics of DC Motor Drive 35
5.2.1 Theoretical Background 35
5.2.2 Simulink Model for Determining Steady-State Parameters 36
5.2.3 Determination of Steady-State Parameters 37
5.3 Dynamic Characteristics of DC Motor Drive 43
5.3.1 Theoretical Background 43
5.3.2 Simulink Model for Dynamic Parameters Determination 46
5.3.3 Inductance Determination 48
5.3.4 Determination of Moment of Inertia 50
5.4 Conclusion 51

Chapter 6. Experiment 5 – DC Motor Control 53
6.1 Introduction 53
6.2 Simulink Model of DC Motor with Current and Speed Controller 53
6.3 Real-Time Implementation of Feed back Control of DC Motor 61
6.4 Conclusion 61

Chapter 7. Experiment 6 – Four-Quadrant Operation of DC Motor 63
7.1 Introduction 63
7.2 Simulink Model of Four-Quadrant Operation of DC Motor 63
7.3 Four-Quadrant Operation of DC Motor in Real-Time 64
7.4 Conclusion 70

Chapter 8. Experiment 7 – Determination of Induction Motor Parameters 71
8.1 Introduction 71
8.2 Theoretical Background 72
8.3 Simulink Model and Real-Time Implementation 75
8.4 Determination of Induction Motor Parameters 77
8.5 Conclusion 81

Chapter 9. Experiment 8 – V/f Speed-Control of Three-Phase Induction Motor 83
9.1 Introduction 83
9.2 Real-Time V/f Speed-Control of Three-Phase Induction Motor 84
9.3 Determination of Torque-Speed Characteristics 86
9.4 Speed-Control of Three-Phase Induction Motor at Constant V/f Ratio 89
9.5 Conclusion 92

Chapter 10. Conclusions and Future Scope of Study 93
10.1 Conclusions 93
10.2 Future Scope of Study 94

References.....**95**

Vita.....**96**

List of Tables

Table 4.1 No-load measurement 32

Table 5.1 Steady–state experimental data 39

Table 5.2 Steady-state parameters 41

Table 5.3 Average values of motor parameters 41

Table 5.4 Steady-state friction model characteristics 42

Table 5.5 Mechanical steady state parameters 42

Table 9.1 Torque-speed characteristics for different supply frequency 87

Table 9.2 Calculated parameter m and c 89

Table 9.3 Average value of slope (m) and intercept (c) 89

Table 9.4 Measured speed values using the slip compensator 92

List of Figures

Figure 1.1 Schematic diagram of DSP based electric-drive system setup 2

Figure 1.2 Motor system 2

Figure 1.3 Power electronics drive board 3

Figure 1.4 CP1104 I/O board 4

Figure 1.5 DSP based electric-drive system 5

Figure 2.1 Rotating mechanical system 8

Figure 2.2 Simulink model for rotating mechanical system 8

Figure 2.3 Simulation parameter settings 9

Figure 2.4 Simulation results 9

Figure 2.5 Simulink model for rotating mechanical system with friction 10

Figure 2.6 Simulation results in steady-state for model including friction 11

Figure 2.7 Simulink model for mechanical system with step changing load 12

Figure 2.8 Simulation results for step changing load 12

Figure 2.9 Simulink model for mechanical system with speed depending load 13

Figure 2.10 Simulation results for speed depending load 13

Figure 3.1 Simulink model of second order system 16

Figure 3.2 Simulation results of second order system 16

Figure 3.3 Real-time Simulink model of second order system 17

Figure 3.4 Control desk layout of second order system 18

Figure 3.5 Real-time simulation settings in Control desk 18

Figure 3.6 Real-time simulation result for slider gain = 1 19

Figure 3.7 Control desk plot for gain = 2.5 19

Figure 3.8 Control desk plot for gain = 0.5 20

Figure 3.9 Control desk plot for gain = 4 20

Figure 4.1 Power-pole as a building block of power electronic converters 23

Figure 4.2 Two-pole converter 23

Figure 4.3 Waveforms during a switching 24

Figure 4.4 Switch mode DC converter for electric-drive 25

Figure 4.5 Simulink model for switching function and duty ratio generation of single-pole converter 26

Figure 4.6 Switching function q_A and duty ratio d_A 27

Figure 4.7 Two-pole converter model 28

Figure 4.8 Two-pole converter model with Vout = +10V 28

Figure 4.9 Two-pole converter model with Vout = -10V 29

Figure. 4.10 Two-pole converter model in real-time 29

Figure 4.11 Real-time model for no-load motor test 31

Figure 4.12 Averaging block 32

Figure 4.13 Current and speed of DC motor at V_motor = 40V displayed in Control desk 33

Figure 4.14 Voltage vs. speed characteristic at no-load 33

Figure 5.1 Machine set model 36

Figure 5.2 Real-time Simulink model for motor and load control 37

Figure 5.3 Control desk layout of real-time Simulink model for motor and load control 38

Figure 5.4 Speed vs. armature current characteristics for motor voltage supplied by different voltages 40

Figure 5.5 Torque-speed characteristic of steady state friction model 42

Figure 5.6 Current response at standstill ($\omega_m = 0$) 44

Figure 5.7 Speed response when the system is made to shut down..... 45
Figure 5.8 Simulink model for dynamic parameter determination..... 47
Figure 5.9 Control desk layout for dynamic parameters determination..... 47
Figure 5.10 Armature current response for a step changed voltage V_M = 3V..... 49
Figure 5.11 Speed of the DC motor when the system is made to shutdown..... 51
Figure 6.1 Simulink model of DC motor..... 54
Figure 6.2 PI current controller..... 55
Figure 6.3 Simulink model of DC motor with current controller..... 55
Figure 6.4 Current waveform for Ia_ref = 1 A..... 56
Figure 6.5 Speed waveform for Ia_ref = 1 A..... 56
Figure 6.6 PI speed controller..... 58
Figure 6.7.a Simulink model of DC motor with cascade control for step changing load..... 58
Figure 6.7.b Simulink model of DC motor with cascade control for constant load..... 58
Figure 6.8 Current waveforms for step change in load..... 59
Figure 6.9 Speed waveforms for step change in load..... 59
Figure 6.10 Current waveforms for step changing speed at constant load..... 60
Figure 6.11 Speed waveforms for step changing speed at constant load..... 60
Figure 6.12 Real-time Simulink model of cascade control of DC motor..... 61
Figure 6.13.a Current controller with external reset..... 62
Figure 6.13.b Speed controller with external reset..... 62
Figure 6.14 Speed and current waveforms for step change in speed..... 62
Figure 7.1 Simulink model for four-quadrant operation of DC motor..... 64
Figure 7.2.a Current and voltage waveforms of four-quadrant operation of DC motor..... 64

Figure 7.2.b Speed waveform of four-quadrant operation of DC motor 65

Figure 7.3 Real-time Simulink model for four-quadrant operation of DC motor 65

Figure 7.4 Speed measurement subsystem 66

Figure 7.5 Speed controller subsystem 66

Figure 7.6 Current controller subsystem 67

Figure 7.7 Duty cycle generation subsystem 67

Figure 7.8 Control desk layout for four-quadrant control of DC motor 68

Figure 7.9 Diagram of four quadrant mode of DC motor operation 69

Figure 7.10 Forward and reverse motoring operation 69

Figure 8.1 Circuit diagram for the characterization of a three phase induction motor 71

Figure 8.2 Per-phase equivalent circuit of three-phase induction motor 72

Figure 8.3 Per-phase equivalent circuit at synchronous speed (s = 0) 73

Figure 8.4 Equivalent circuit of induction motor: (a) – for rated condition,
(b) – for blocked rotor test 74

Figure 8.5 Simulink model for characterization of induction motor 76

Figure 8.6 Duty cycle generation of three-phase induction motor 77

Figure 8.7 Control desk layout for motor parameters determination 78

Figure 8.8 Voltage and current waveforms at synchronous speed 79

Figure 8.9 Voltage and current waveforms of blocked rotor test 81

Figure 9.1 Real-time Simulink model for V/f speed-control of induction motor 84

Figure 9.2 Simulink model of f_ref_slip_comp sub-system block 85

Figure 9.3 Control desk layout for V/f speed control of induction motor 85

Figure 9.4 Machine set model 86

Figure 9.5 Torque-speed characteristics for different f_ref 88

Figure 9.6 Machine set model for speed-control of induction motor..... 90

Abstract

This thesis refers to the EE 4490 Adjustable Speed Drives course, which is taught at Louisiana State University (LSU). The part of this course is variable speed AC and DC drives laboratory.

The objective of this thesis is to modify the existing DSP Based Electric Drives Lab Manual developed by Department of Electrical and Computer Engineering, University of Minnesota in order to adjust it to the EE 4490 course syllabus and to verify the experiments by carrying out the tests on the lab equipment available at the Elec. & Comp. Eng. Dept at LSU.

There are four major components, of the available lab equipment, which are used to perform all the lab experiments: Motor Coupling System, Power Electronics Drive board, DSP based DS1104 R&D controller and CP 1104 I/O board.

The DS1104 R&D controller is programmed applying the Matlab/Simulink software and with the use of CP 1104 I/O board and Power Electronics Drive board the motor-load set is controlled.

The thesis consists of two parts:

- EE 4490 Adjustable Speed Drives Laboratory based on dSPACE controller Lab Manual,
- Lab Report.

The first part gives students the detailed introduction to lab experiments. The second part contains the results obtained from the experiments.

The lab manual consists of eight experiments:

- The first two experiments: Expt. 1 and Expt. 2 introduce students to modeling the dynamics of the system in Simulink (Expt. 1) and next, to model it in real-time and to

perform the experiment using the dSPACE controller together with the Control desk (Expt. 2).

- The Experiments 3 – 6 allow to learn students how to design the current and speed controllers for DC PM motor drive, to test them by modeling the whole DC drive system in Simulink and next, to control the system in real-time.
- The last two experiments (Expts. 7 and 8) concern the characterization and V/f speed control of induction motor.

By performing all lab experiments students can learn how to build simple dynamic model in Simulink/Matlab to more complex systems such as feed-back control of DC motor drive and V/f speed control of induction motor.

Chapter 1

Introduction

1.1 Overview of the Thesis

The thesis project relates directly to the EE 4490 course, Adjustable Speed Drives, which is taught at Louisiana State University. According to the Catalog Data this course offers 2 hrs. lecture and 2 hrs. lab.

Referring to the Course Syllabus the course objectives are:

The course will give students a basic knowledge about electric drives based on DC and AC motors. The speed control of electric motors accomplished by power electronic converters (controlled rectifiers and inverters) will be analyzed using the computer simulation. Students will learn how to design electric drives with speed, position and torque controllers. A practical implementation of designed controllers will be during the lab experiments.

The study objects of this course are electric drives based on DC and AC motors. The main objective of this course is a speed control. It will be accomplished by power electronics converters and speed controllers. The lab experiments, which are the integral part of the course, are focused on practical implementation of controllers earlier designed and tuned using Matlab/Simulink.

The electric drive system is based on DSP controller and there are four major components (see Fig. 1.1), which will be used to perform all the experiments in this course:

- **Motor coupling system** (Fig. 1.2)

  This system contains the motor that need to be characterized/controlled. The system has a mechanical coupling arrangement to couple two electrical machines. The motor under test or whose speed/torque needs to be controlled could be either a DC motor or three-

phase induction motor. The system also has an encoder mounted on the machine to measure the speed. It can be used for closed loop feedback speed control of the motor. The motor demands a controlled pulse-width modulated (PWM) voltage to run at desired speed or torque.

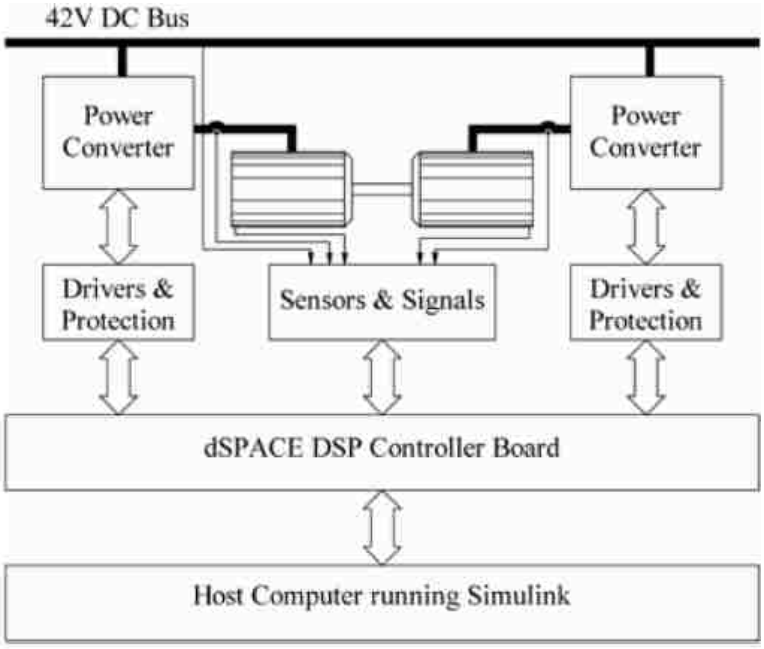

Figure 1.1 Schematic diagram of DSP based electric-drive system setup [3]

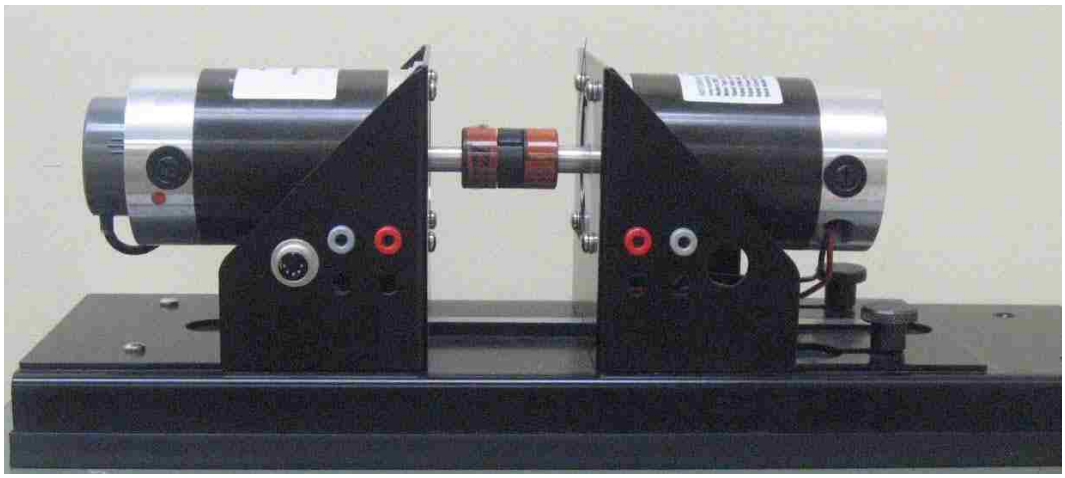

Figure 1.2 Motor system

- **Power Electronics Drive Board** (Fig. 1.3)

  This board has the capability to generate two independent PWM voltage sources (A1 B1 C1 and A2 B2 C2) from a constant DC voltage source. Hence, two machines can be controlled independently for independent control variables, at the same time. This board also provides the signals of phase currents, DC bus voltage etc. to control the motor for a desired speed or torque. In order to generate the controlled PWM voltage source, this board requires various digital control signals. These control signals dictates the magnitude and phase of the PWM voltage source. They are generated by the DS1104 R&D controller board inside the computer.

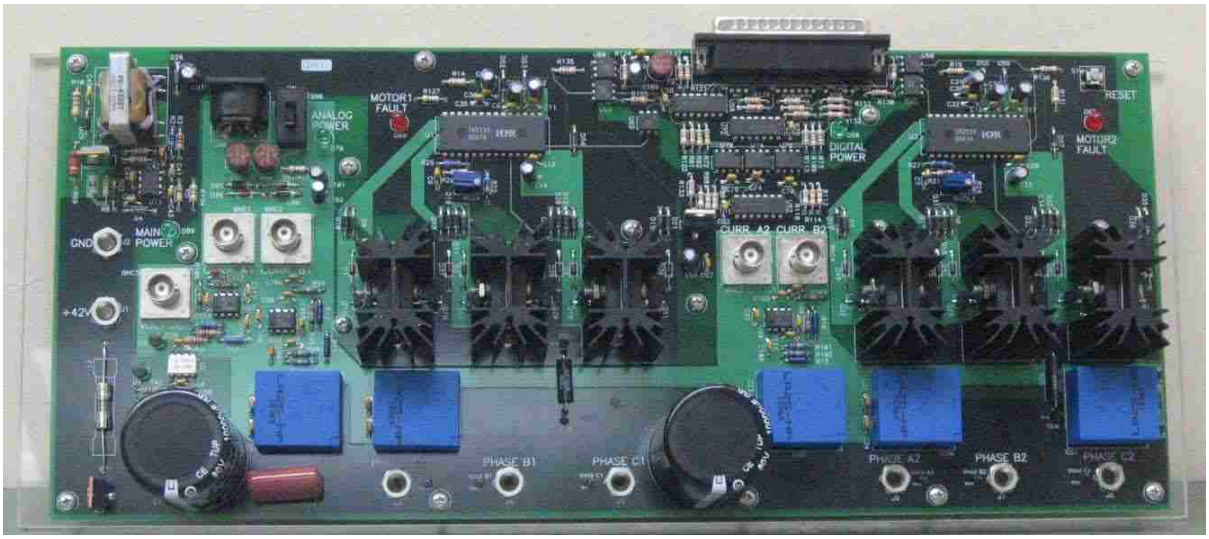

Figure 1.3 Power electronics drive board

- **DSP based DS1104 R&D controller card and CP 1104 I/O board** (Fig. 1.4)

  In each discrete-time step, the DS1104 controller card takes some action to generate the digital control signals. The type of action is governed by what we have programmed in this board with the help of Matlab/Simulink real-time interface. This board monitors the input (i.e. motor current, speed, voltage etc.) with the help of the CP1104 I/O board in

each discrete-time step. Based on the inputs and the variables that need to be controlled (i.e. motor speed or torque) it takes the programmed action to generate the controlled digital signals. The CP1104 I/O board is an input-output interface board between the Power Electronics drives board and also, speed signal (from encoder) from motor coupling system, to the DS1104 controller card. In turn, the controlled digital signals supplied by DS1104 controller card are taken to the Power Electronics drives board by CP1104.

Figure 1.4 CP1104 I/O board

- **Matlab/Simulink and Control desk (Programming DS1104 and control in real-time)**

  Simulink is a software program with which one can do model-based design. The I/O ports of CP1104 are accessible from inside the Simulink Library browser. Creating a program in Simulink and procedure to use the I/O port of CP 1104 will be detailed in experiments. When the Simulink model is built in real-time the model is converted into a real-time system on hardware (DS1104). Simulink generates a *.sdf file when the model is converted into real-time. This file gives access to the variables of Simulink model in Control Desk software. In this software a control panel can be created, which allow changing the variables of Simulink model in real-time in order to communicate with

DS1104, and hence, can change the reference quantities such as speed or torque of the motor.

The whole DSP-based electric drives system is shown in Fig. 1.5

The laboratory system was designed at the Department of Electrical and Computer Engineering, University of Minnesota. The group conducted by Prof. Ned Mohan designed the lab experiments and wrote the Lab Manual [3]. The aim of this project is to adapt this manual to the needs of the EE 4490 course these experiments by modifying it and by verifying the experiments using the available in the ECE Department lab equipment.

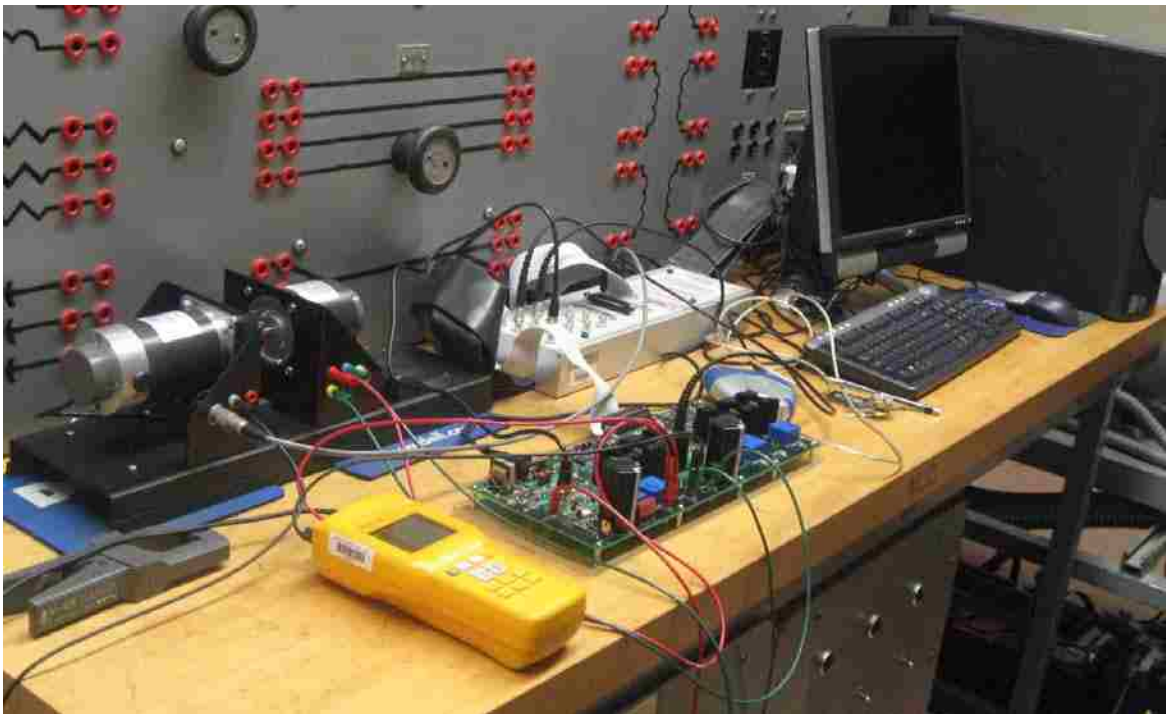

Figure 1.5 DSP based electric-drive system

1.2 Objectives of the Thesis

- To modify the existing DSP-Based Electric Drives Lab Manual in order to adapt it to the EE 4490 course syllabus.
- To verify the experiments by carrying out the tests on the available lab equipment.

1.3 Outline of the Thesis

The Thesis consists of two parts:

- **Lab Manual** to EE 4490 Adjustable Speed Drives course
- **Thesis**

The first part is primarily based on DSP Based Electric Drives Laboratory User Manual prepared by the Department of Electrical and Computer Engineering at University of Minnesota, and which was adapted to the needs of EE 4490 course – Adjustable Speed Drives, which is taught at Electrical and Computer Engineering Department, Louisiana State University.

The second part (this thesis) is the lab report on the eight experiments carried out on the DC and AC drives. In both the parts the first two experiments: Experiment 1 and Experiment 2 introduce the users to Matlab/Simulink modeling and DSP programming of electric drives. The Experiments 3 – 6 are on modeling and testing of DC variable speed drives based on PM DC motors. The last Experiments 7 and 8 concern the induction motor speed control

The Thesis ends with the conclusions deducted from the lab experiments.

Chapter 2

Experiment 1 – Building a Simple Dynamic Model in Simulink

2.1 Introduction

Simulink tool in Matlab helps to represent the dynamic problem using interconnected blocks and has the capability to view the solution using graphs and plots. In this experiment using Simulink a continuous time system is built in graphical way using interconnected blocks. This system helps to understand the mechanical interactions of the rotating system consisting of a motor and load.

2.2 Theoretical Background

A simple model of rotating mechanical system is developed for the following set of equations with the help of Simulink tool in Matlab [1]:

– inertia torque

$$T_J = T_M - T_L \tag{2.1}$$

– equivalent moment of inertia

$$J_{eq} = J_M + J_L \tag{2.2}$$

– acceleration

$$a = \frac{T_J}{J_{eq}} \tag{2.3}$$

– angular speed

$$\omega_m = \int a \,.\, dt \tag{2.4}$$

– rotor position

$$\theta = \int \omega_m \,.\, dt \tag{2.5}$$

These equations constitute the motion equation:

$$T_M = T_J + T_L\,, \tag{2.6}$$

which represent the rotating system shown schematically in Fig. 2.1

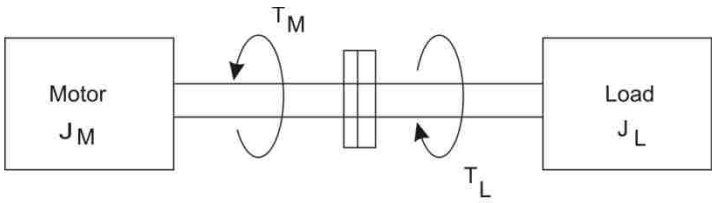

Figure 2.1 Rotating mechanical system

2.3 Modeling a Mechanical System in Simulink

2.3.1 Simulink Model with Inertia Only

Fig. 2.2 shows the Simulink model for rotating mechanical system. The simulation parameters for this system are shown in Fig. 2.3. The Slider Gain values for this model are presented in Fig. 2.2. The fixed step size is 0.001 so from 0 to 1 second the total number of steps carried is 1000. The inertia of the mechanical system has $J_{eq} = 0.058$ kg·m^2. The output for the Simulink model is shown in Fig. 2.4.

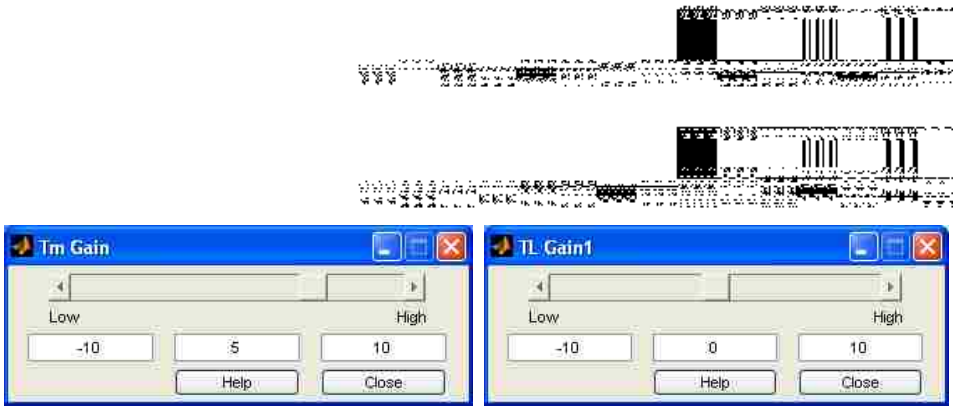

Figure 2.2 Simulink model for rotating mechanical system

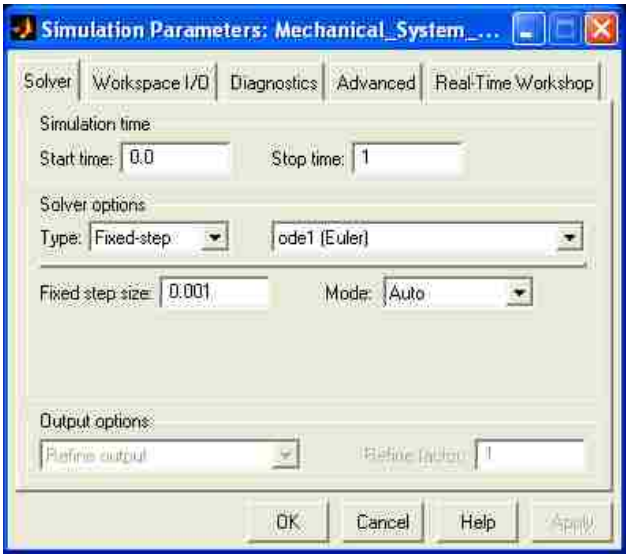

Figure 2.3 Simulation parameter settings

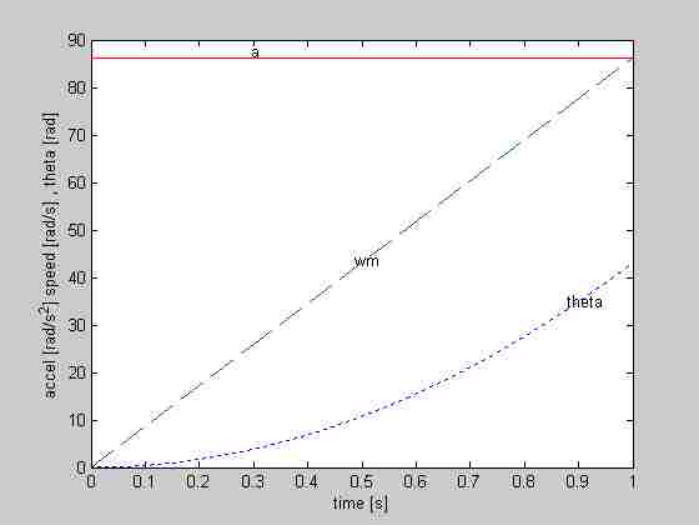

Figure 2.4 Simulation results

By changing the Slider Gain's of the Simulink model shown in Fig. 2.2 we adjust the motor torque T_M and load torque T_L and observe the following variations:

- if we make the Slider Gain values as $T_M = T_L$ then $w_m = 0$,
- if we make the Slider Gain values as $T_M > T_L$ then $w_m > 0$,
- if we make the Slider Gain values as $T_M < T_L$ then $w_m < 0$.

2.3.2 Mechanical Model with Friction

When the friction is included in the system in the form of the friction torque:

$$T_{fric} = B \cdot \omega \tag{2.7}$$

the motion equation of the rotating system has the form

$$T_M = J_{eq} \frac{d\omega_m}{dt} + B \cdot \omega + T_L \tag{2.8}$$

The Simulink model with friction is shown in Fig. 2.5. In the model a **Sine** block is included in order to obtain the angular displacement value repeating instead of continuously increasing or decreasing. In order to show the system operating continuously the **stop time** in **simulation parameters** is changed to **"inf"** instead of one second.

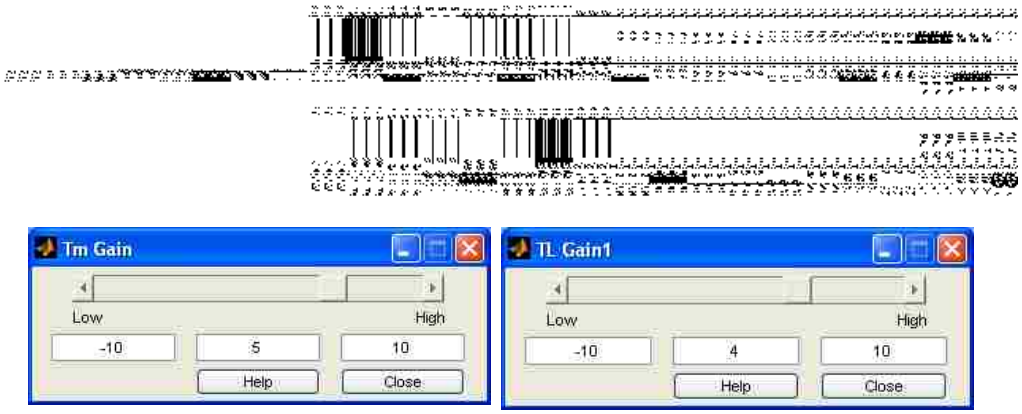

Figure 2.5 Simulink model for rotating mechanical system with friction

The output of the simulation is shown in Fig 2.6.

As it is seen the addition of friction to the system makes the speed constant. It does not increase or decrease. It gained stability and the angular displacement is repeating. In general the frictional torque (see Eqn. 2.8) reduces the rotational speed. When the Slider Gain value of motor torque is

larger than the Slider Gain value of load torque we will have constant positive overall torque in the direction of the motor speed. When the Slider Gain value of load torque is larger than the Slider Gain value of motor torque then, we will have a negative overall torque with the motor speed in negative direction.

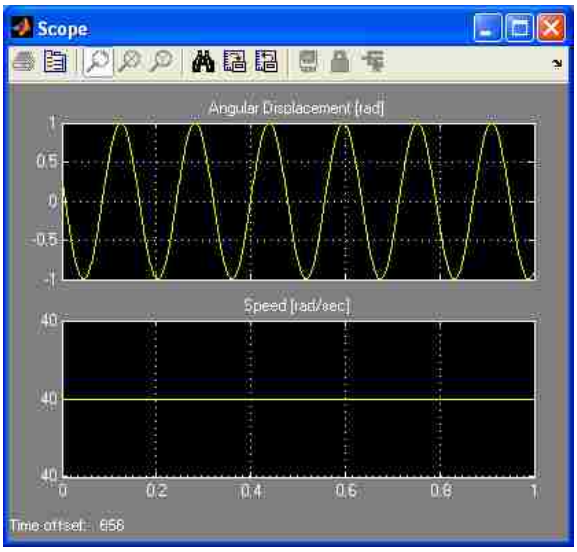

Figure 2.6 Simulation results in steady-state for model including friction

2.3.3 Mechanical System with Modified Load

– Model with step-changing load

The mechanical model shown in the Fig. 2.7 consists of a load changing in step. The **Step** block from the Simulink Sources library is used as the load. This block has the following parameters:

- Step time – 1.5 s
- Initial value – 0 N·m
- Final value – 5 N·m

The simulation time is 3 seconds and the friction coefficient $B = 0.35 \left[{}^{N.m}/_{rad/s} \right]$. The simulation results for the step changing load is shown in Fig. 2.8.

Figure 2.7 Simulink model for mechanical system with step changing load

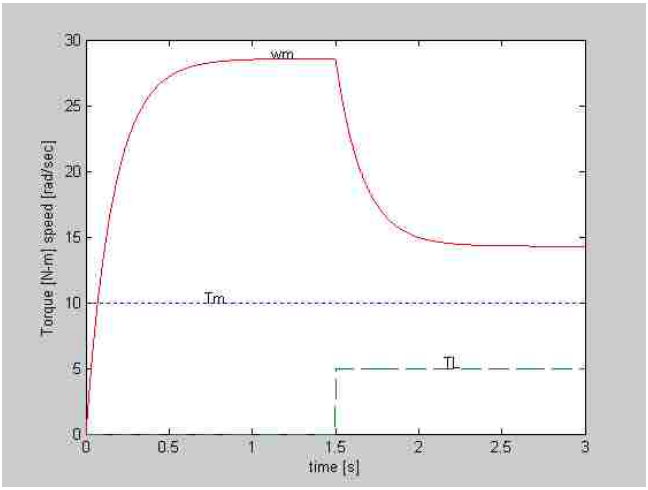

Figure 2.8 Simulation results for step changing load

From the Fig. 2.8 one can see that when the load torque is changed from 0 to 5 N·m at 1.5 seconds the speed of the mechanical system is decreased from 28.5 to 14.5 [rad/sec]. During the interval from 0 to 1sec the load torque + friction torque are smaller than motor torque, so why the system accelerates till $T_L + T_{fric} = T_M$. The transition period is also present when the load torque has increased after 1.5 s.

– Model with Speed Depending Load

In this model the load torque depends on the speed according to equation:

$$T_L = k{\omega_m}^2 \tag{2.9}$$

The Simulink model for the speed-depending load is shown in Fig. 2.9. The **Function** block from the Continuous library with the function as in Eqn. 2.9 is used as a load torque.

Figure 2.9 Simulink model for mechanical system with speed depending load

The simulation results for the speed depending load shown in Fig. 2.10 have the simulation time of 0.3 seconds. During this time the system has reached steady state. In this case the motor torque is higher than the load torque and the system accelerates. The system reaches the steady-state when the load torque + friction torque became equal to the motor torque.

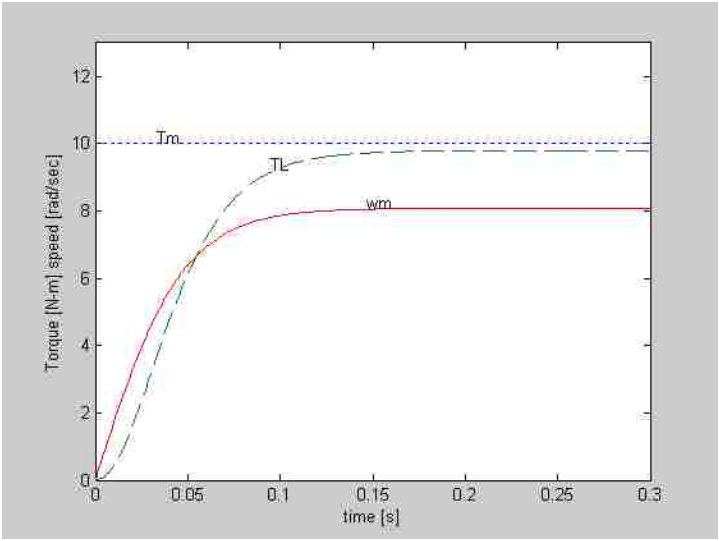

Figure 2.10 Simulation results for speed depending load

2.4 Conclusion

In this experiment, first the Simulink model of rotating mechanical system without friction was examined. Next, the Simulink model with frictional torque was studied, and finally, the mechanical system with step-changing and with speed-depending loads was analyzed. From the analysis carried out for 4 versions of rotating mechanical system, the following conclusions can be deduced:

- The system without friction and with motor torque greater than load torque is moving with the linear rising speed.
- If the friction is added to the system it reaches steady–state after initial acceleration and it is moving with a constant speed.
- When the load of constant torque is added after the system reached the constant speed, its speed goes down and finally the motor is moving with lower constant speed.
- When the load torque depends on speed, as it is in pumps and fans, the whole system after starting up, is running with the constant speed at which driving torque of the motor is equal to the load and friction torque according to the equation $T_M = k{\omega_m}^2 + B\omega_m$.

Chapter 3

Experiment 2 – Building a Simple Real-Time Model in Simulink

3.1 Introduction

In this Experiment a Simple Real-time Model of Second Order System is built using Simulink tool in Matlab and dSPACE. Initially the graphical model is built in Simulink and after verifying the results the model is implemented in real-time replacing some of the Simulink blocks with real-time equipment (i.e. Function Generator and Oscilloscope)

3.2 Model Description

In this Experiment the Simulink/Real-time model is represented by a second order transfer function, in which the input to the transfer function is a square wave with amplitude of 1V and frequency of 2 Hz.

For the Simulink model of second order system **Signal Generator** from **Sources** library is served as an input and **Scope** from **Sinks** library is used to observe the output waveforms.

For the real-time model of second order system a real function generator is served as an input and oscilloscope is used to observe the waveforms of second order system.

The transfer function of the second order system is represented by following equation [2]:

$$G(s) = \frac{{\omega_n}^2}{s^2 + 2\xi\omega_n s + {\omega_n}^2} \tag{3.1}$$

For the frequency $f = 20\,Hz$ and damping coefficient $\xi = 0.7$ the angular frequency $\omega_n = 2\pi f = 125.6\,rad/s$ and the transfer function takes the form:

$$G(s) = \frac{15{,}790.43}{s^2 + 175.92s + 15{,}790.43} \tag{3.2}$$

3.3 Simulation in Simulink

The second-order system described by Eqn. 3.2 is represented by the Simulink block diagram shown in Fig. 3.1. The simulation parameters in the **Solver** are set as follows:

- Stop time – 2 seconds
- Type – Fixed-step
- Solver – ode1 (Euler)
- Fixed-step size – 0.001

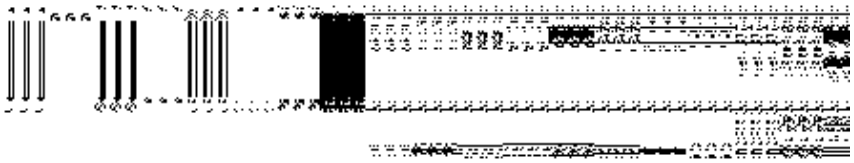

Figure 3.1 Simulink model of second order system

The input of the transfer function is a square wave from the **Signal Generator**. The output and input signals recorded by the scope are shown in Fig. 3.2. The output signal follows the input with delay. Some small overshoot is visible in the output signal waveform.

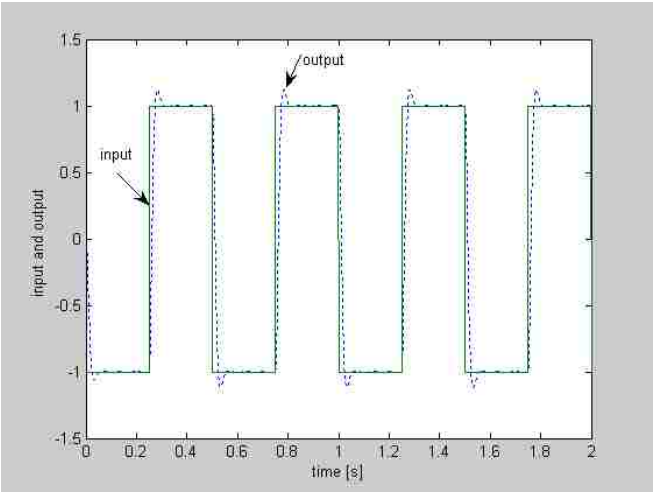

Figure 3.2 Simulation results of second order system

3.4 Real-Time Modeling Using dSPACE

The analyzed second order system modeled in real-time Simulink is shown in Fig. 3.3. In this model the Signal Generator block is replaced by **DS1104ADC_C5** got from the dSPACE library and it converts analog signal into digital one. The Simulink **Scope** block is replaced by **DS1104DAC_C1** block that converts the digital into analog signal. These two blocks allow to connect the external analog devices to the Simulink transfer function block with digital signals.

It means, the real function generator is connected to DS1104ADC_C5 and a real Oscilloscope to DS1104DAC_C1 block.

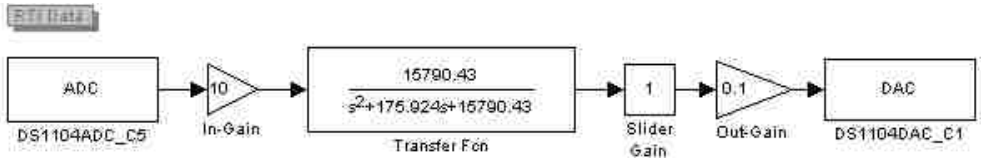

Figure 3.3 Real-time Simulink model of second order system

To implement a model in real-time the model should run continuously, so the **Stop** time for the real-time Simulink model is set to **"inf"**. Next, the Simulink model shown in Fig. 3.3 is converted into the real-time **DSP** code with the help of **build model** in **Matlab/Simulink>Tools**. After building the model the DSP code is exported to dSPACE and implemented in CP1104 using Control Desk software. This software provides Graphical User Interface (GUI) in which the input and output waveforms are graphically viewed.

The **Slider Gain** and **Data Acquisition** plotter (Scope) blocks in Virtual Instruments of dSPACE Control Desk software is used to vary the real-time gain and view the Input and Output signals (to and from of second order system). The Fig. 3.4 presents the Control Desk layout for second order system. Settings of the capture window for the real-time simulation in Control Desk software is shown in Fig. 3.5.

The real-time simulation results are shown in Fig. 3.6

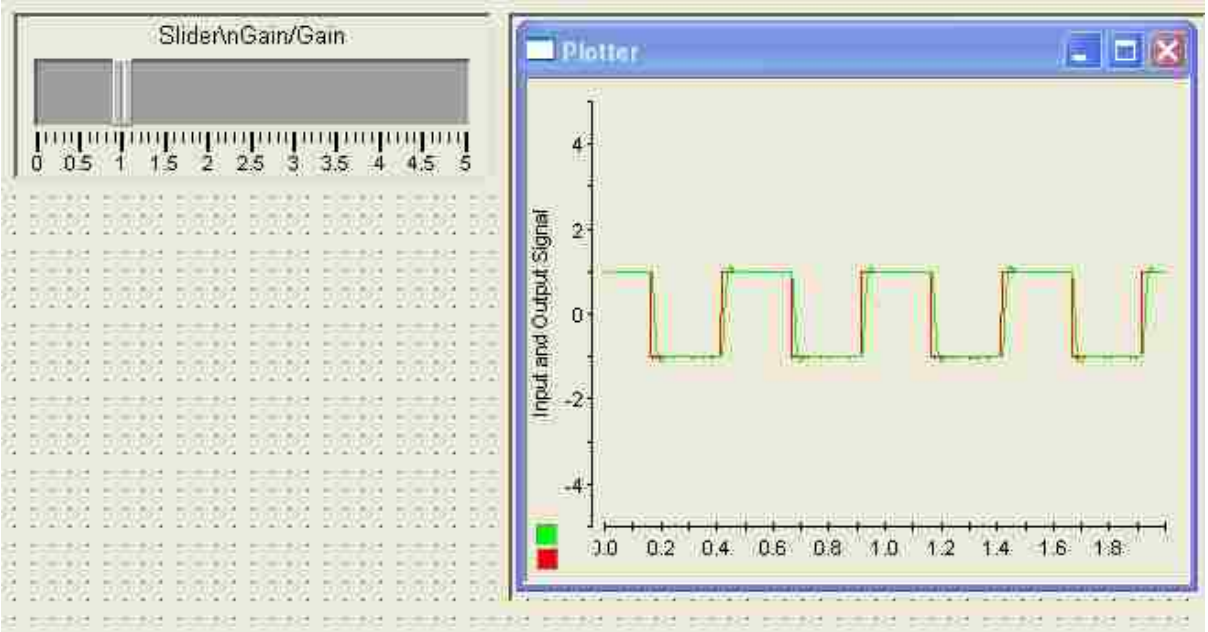

Figure 3.4 Control desk layout of second order system

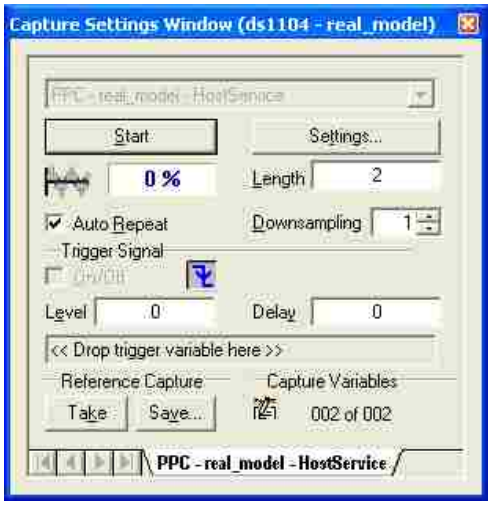

Figure 3.5 Real-time simulation settings in Control desk

The overshoot value of real-time plot seen in Fig. 3.6 is of same magnitude as that in Fig. 3.2 obtained from Simulink model. In Fig. 3.7 the gain was increased to 2.5 times unity. The input waveform has the magnitude of 1V at the top and -1V at the bottom. The output waveform (observed in Control Desk) of Fig. 3.7 has an overshoot of **2.5V** and **-2.5V** and it reached to a

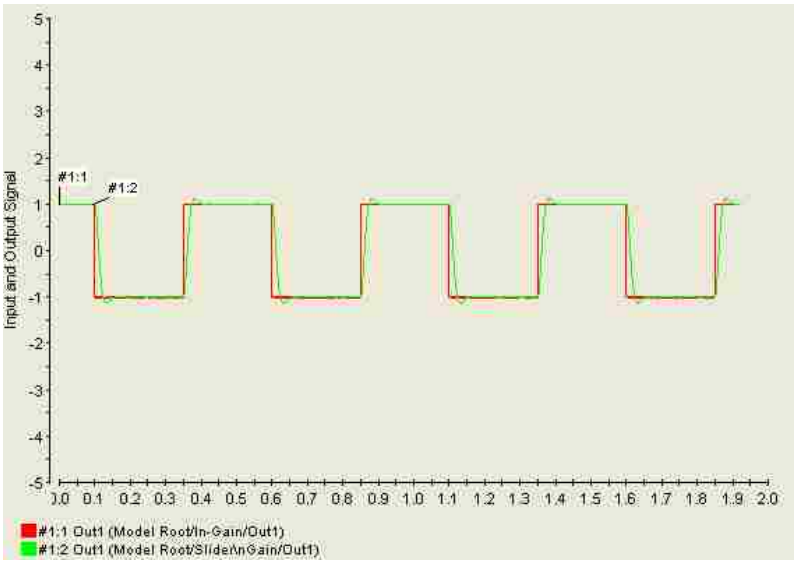

Figure 3.6 Real-time simulation result for slider gain = 1

steady state value of +/- 2.25V. This waveform observed in Oscilloscope (which is connected to DS1104DAC_C1) has the steady state values of +/- 2.5V. Thus, comparing the simulation results (i.e. in Control Desk) with real-time results (i.e. in Oscilloscope) we see that Control Desk software does not give the exact graphical output.

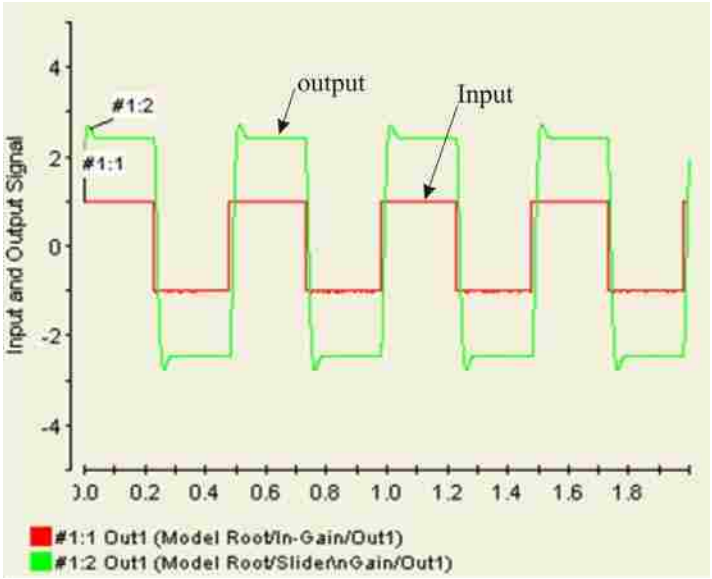

Figure 3.7 Control desk plot for gain = 2.5

For the results shown in Fig. 3.8 the gain was lowered to 0.5 times unity. The output waveform was not exactly the Square wave.

Fig. 3.9 shows the waveforms with the slider gain increased to 4 times.

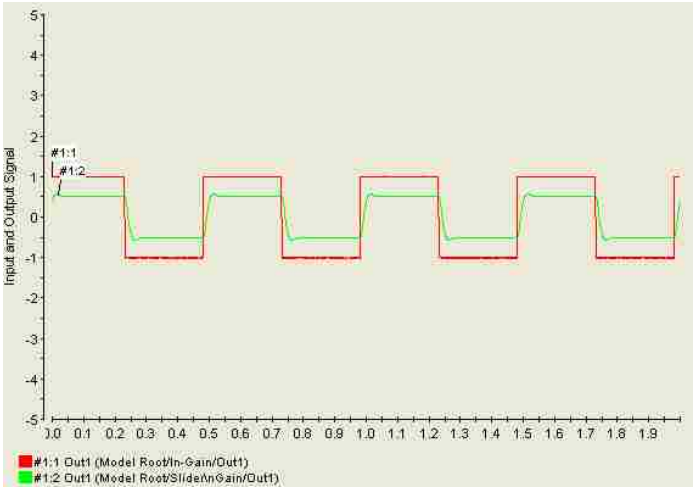

Figure 3.8 Control desk plot for gain = 0.5

In Fig. 3.9 the overshoot of the output signal is larger but the stabilization gives the plot a Square wave appearance. For this gain value the waveform in Oscilloscope has the same steady state value as of Control Desk plot with +/- 4V amplitude.

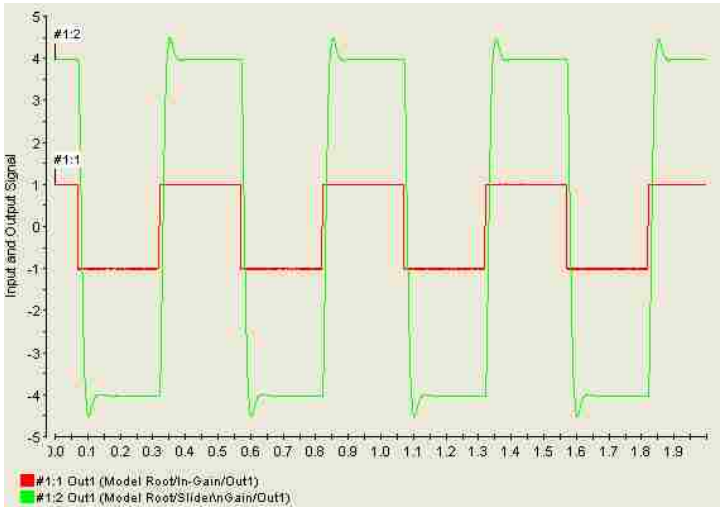

Figure 3.9 Control desk plot for gain = 4

3.5 Conclusion

In this experiment the Simulink model of second order system was built first. Next, the same model was analyzed in the real-time with the help of dSPACE Control Desk. In the real-time model the second order transfer function was supplied with real Signal Generator and the output was viewed in real oscilloscope. The dSPACE Control Desk was allowed to control the output signal measured by oscilloscope.

Comparing the output results obtained from Simulink with the Oscilloscope output signal only minor difference was observed.

Chapter 4

Experiment 3 – Switch-Mode DC Converter and No-Load DC Motor Test

4.1 Introduction

In this experiment with the help of Matlab modeling tool Simulink and dSPACE the Switch-Mode DC Converter is built in real-time to control the output voltage of the controller using PWM algorithm. First, the Simulink model of Switch-Mode DC Converter (i.e. Single-Pole and Two-Pole Converter Model) is built and, after verifying the results, it is implemented in real-time. Next, a DC motor is connected to the output terminals (i.e. Phase A1 and Phase B1) of the Power Electronics Board such that a variable voltage is applied to the terminals of DC motor. Now, by changing the magnitude of the applied voltage, the speed of the motor is varied. This is also referred to as an open-loop voltage control of DC motor.

4.2 Theoretical Background

The switch-mode converter will be built on the basis of bi-positional switch, which constitutes a power pole as shown Fig. 4.1. The converter for DC motor drives consists of two such poles (Fig. 4.2), whereas DC-to-three phase AC converter consists of 3 such poles [4]. In Fig. 4.1 the output pole-voltage, $v_{AN}(t)$ is either V_d (input voltage) or 0 depending upon the position of the bi-positional switch.

The output pole-voltage $v_{AN}(t)$ of the power-pole is a switching waveform (Fig. 4.3) whose value alternates between V_d and 0 depending on the pole switching function $q_A(t)$ [4]:

$$v_{AN}(t) = q_A(t)V_d \tag{4.1}$$

The average output voltage $\bar{V}_{AN}$ of the power-pole can be controlled by changing the pulse width of the pole switching function $q_A(t)$ (see Fig.4.1).

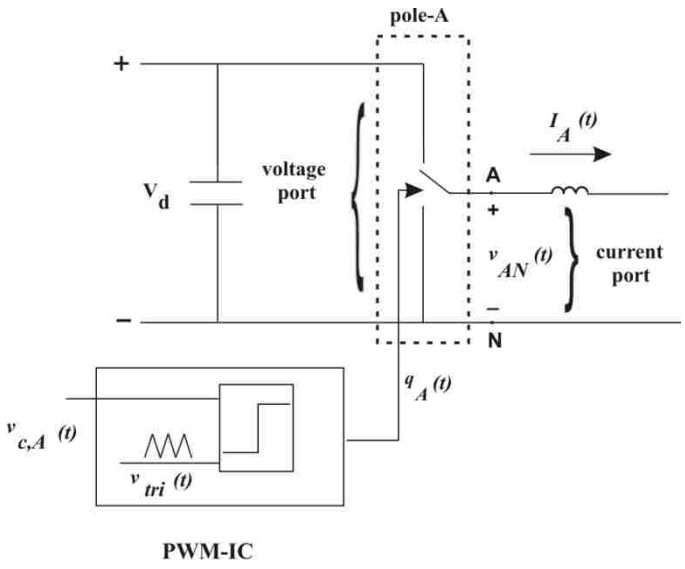

Figure 4.1 Power-pole as a building block of power electronic converters [4]

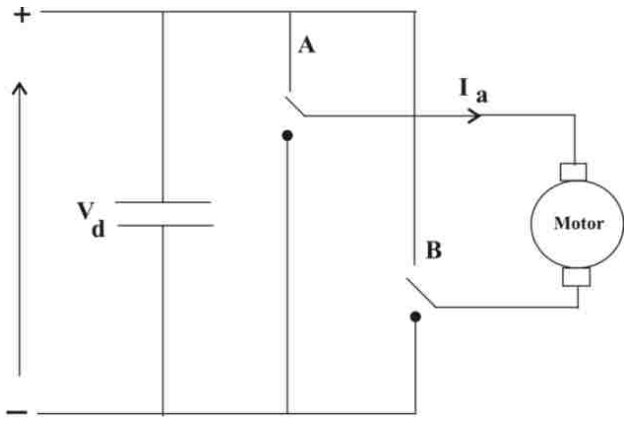

Figure 4.2 Two-pole converter

4.2.1 Pulse Width Modulation (PWM) of Switching Power Pole

Controlling the pulse width of the pole switching function $q_A(t)$ can be accomplished using a technique called Pulse Width Modulation (PWM). In this technique a control voltage $v_{c,A}(t)$ is compared with triangular waveform signal to obtain pole switching function $q_A(t)$ (Fig. 4.3):

$$\left.\begin{array}{l} if\ v_{c,A}(t) > V_{tri}(t) \Longrightarrow q_A(t) = 1 \\ if\ \ v_{c,A}(t) < V_{tri}(t) \Longrightarrow q_A(t) = 0 \end{array}\right\} \quad (4.2)$$

The average output voltage of the power-pole with respect to duty ratio over one switching cycle is given by:

$$\bar{v}_{AN}(t) = d_A(t)V_d \tag{4.3}$$

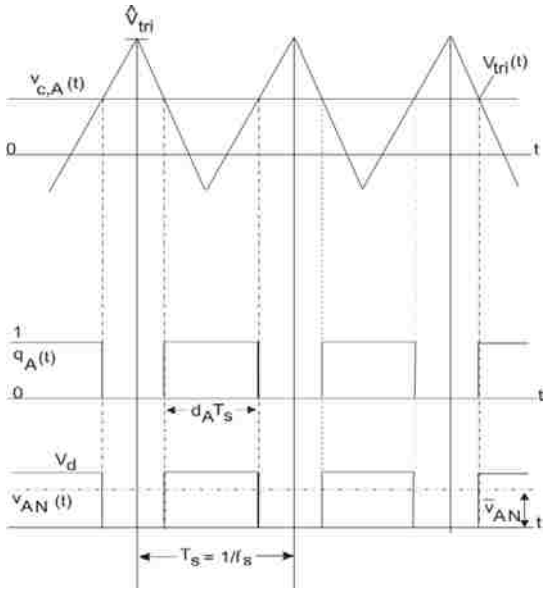

Figure 4.3 Waveforms during a switching [4]

4.2.2 Duty Ratio and Switching Function of Single-Pole Converter

The duty ratio for a single PWM pole is given by the equation [4]:

$$d_A(t) = \frac{1}{2} + \frac{1}{2}\frac{v_{c,A}(t)}{\hat{V}_{tri}} \tag{4.4}$$

Solving the equations (4.2) and (4.3) for $\hat{V}_{tri} = 1V$ we obtain:

$$v_{c,A}(t) = \frac{2\bar{v}_{AN}(t)}{V_d} - 1 \tag{4.5}$$

4.2.3 Two-Pole Converter Model

In two pole converter model the average output voltage $\bar{v}_o(t)$ can be positive or negative. The DC converter consists of two switching power poles (Fig. 4.1.a). The converter average output voltage is the difference between the two pole output voltages, measured with respect to the DC bus ground.

$$\bar{v}_o(t) = \bar{v}_{AB}(t) = \bar{v}_{AN}(t) - \bar{v}_{BN}(t) \tag{4.6}$$

At any given instant of time, the control voltages for the two poles are complimentary, i.e.

$$v_{c,A}(t) = -v_{c,B}(t) \tag{4.7}$$

By solving Eqn. 4.1 through Eqn. 4.7, we can write

$$v_{c,A}(t) = -v_{c,B}(t) = \frac{\bar{v}_{AB}(t)}{V_d} \tag{4.8}$$

$$d_A(t) = \frac{1}{2}\left(v_{c,A}(t) + 1\right) \tag{4.9}$$

$$d_B(t) = \frac{1}{2}\left(-v_{c,A}(t) + 1\right) \tag{4.10}$$

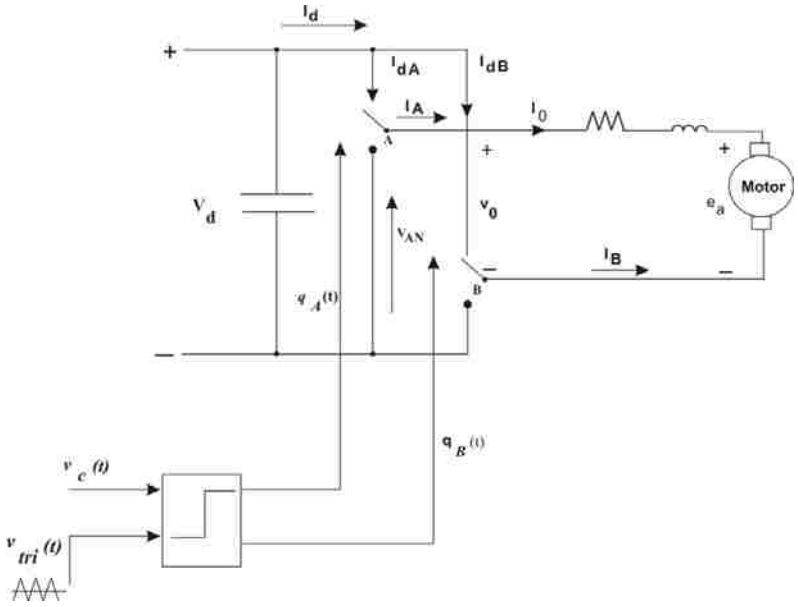

Figure 4.4 Switch mode DC converter for electric-drive [4]

4.3 Simulation of Switch-Mode Converter in Simulink

4.3.1 Simulink Model for Single-Pole Converter

The Eqns. (4.4) and (4.5) are implemented in the Simulink to obtain the duty ratio and switching function for the single pole converter model.

The Fig. 4.5 shows the Simulink block diagram for the single pole converter model with the **simulation parameters** mentioned as **solver** options:

- Stop time: 0.002
- Type: Fixed-step
- Solver: ode1 (Euler)
- Fixed-step size: 0.000001

The control voltage $v_{c,A}(t)$ is compared with triangular waveform using a **Relay** block. The output of relay is set to 1 if the difference between control voltage and triangular signal is positive, otherwise 0. The **Slider Gain** has the block properties shown in Fig. 4.5. The values of DC bus voltage (Vd = 42) and switching frequency (fsw = 10000) are set at the Matlab command prompt before the simulation.

The duty ratio and switching function waveforms of single-pole converter model after the simulation are shown in Fig. 4.6.

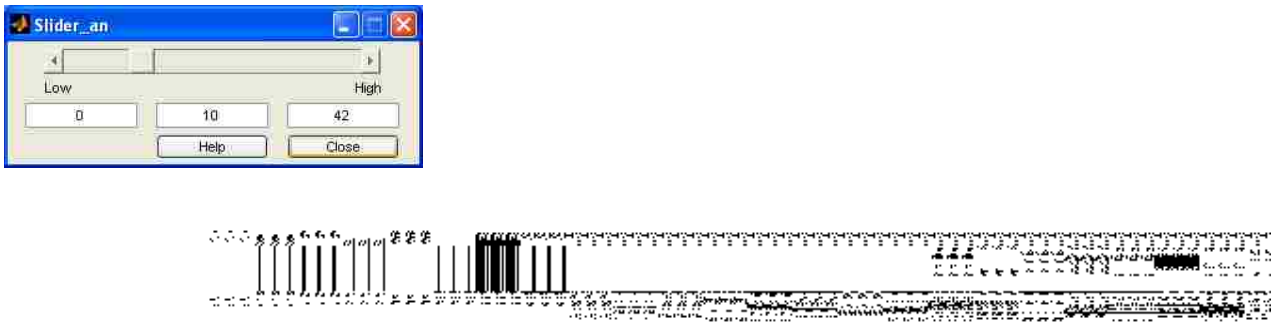

Figure 4.5 Simulink model for switching function and duty ratio generation of single-pole converter

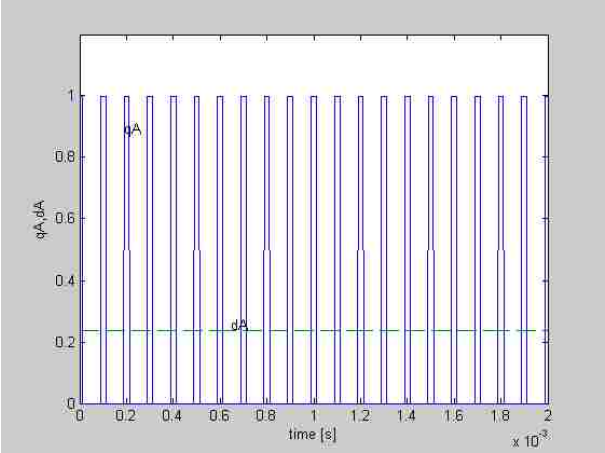

Figure 4.6 Switching function q_A and duty ratio d_A

4.3.2 Simulink Model for Two-Pole Converter

The Simulink model of two pole converter is the comparison of two control voltages $v_{c,A}(t)$ and $v_{c,B}(t)$ with triangular waveform. The Eqn. (4.8) describes the control voltages of the two-pole converter model. The Eqns. (4.8), (4.9), and (4.10) are implemented in Simulink to determine the duty ratios and switching functions of two pole converter. Fig. 4.7 shows the two pole converter model. In this figure power poles are modeled using the **Switch** block. The **Relay** block provides the switching functions for the poles q_A and q_B.

The simulation parameters and the variables of Fig. 4.7 are set as in section 4.3.1.

In the two-pole converter model the output voltage is determined with two slider gain values. Fig. 4.8 presents the output voltage and duty ratios when the slider gain was set to positive value. In the Fig. 4.9 the output voltage and duty ratios are calculated when the slider gain value was set to negative value.

4.3.3 Implementation of Two-Pole Converter Model in Real-Time

After obtaining the results of duty ratios and output voltage for the two-pole converter in the Simulink, this converter is implemented in the real-time on DS1104 controller board.

In the real-time model the converter output voltage can be controlled with the help of dSPACE control-desk.

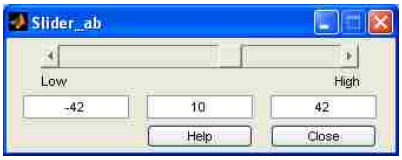

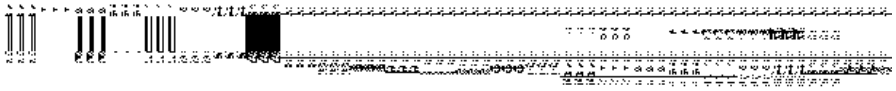

Figure 4.7 Two-pole converter model

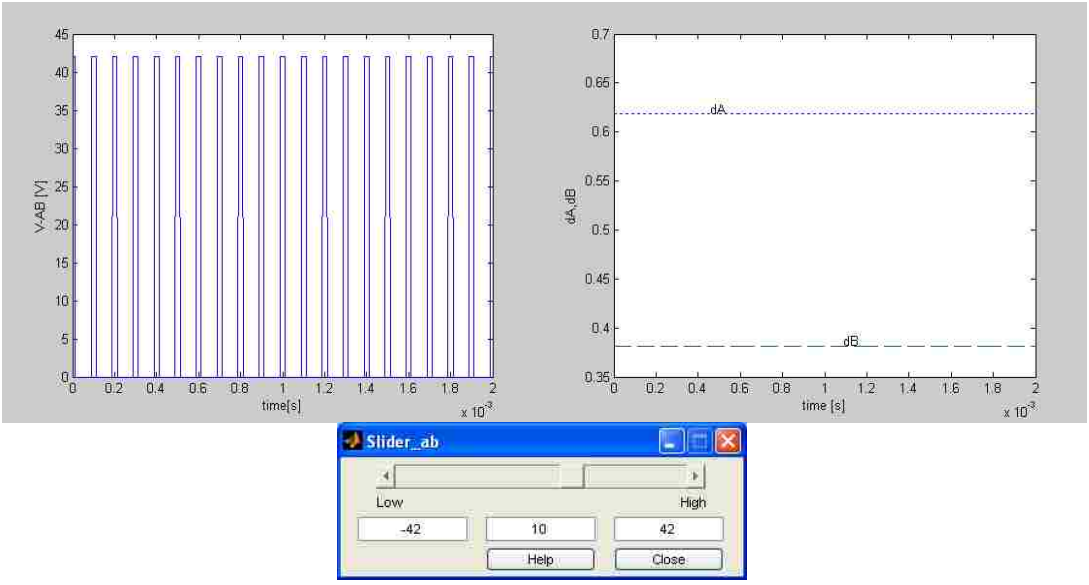

Figure 4.8 Two-pole converter model with Vout = +10V

The triangular waveform generator and the comparator for all the converter poles of Fig. 4.7 can be replaced with **DS1104SL_DSP_PWM3** block provided by dSPACE. The duty ratios are served as the inputs to **DS1104SL_DSP_PWM3**. The Fig. 4.10 presents the two-pole converter model in real-time.

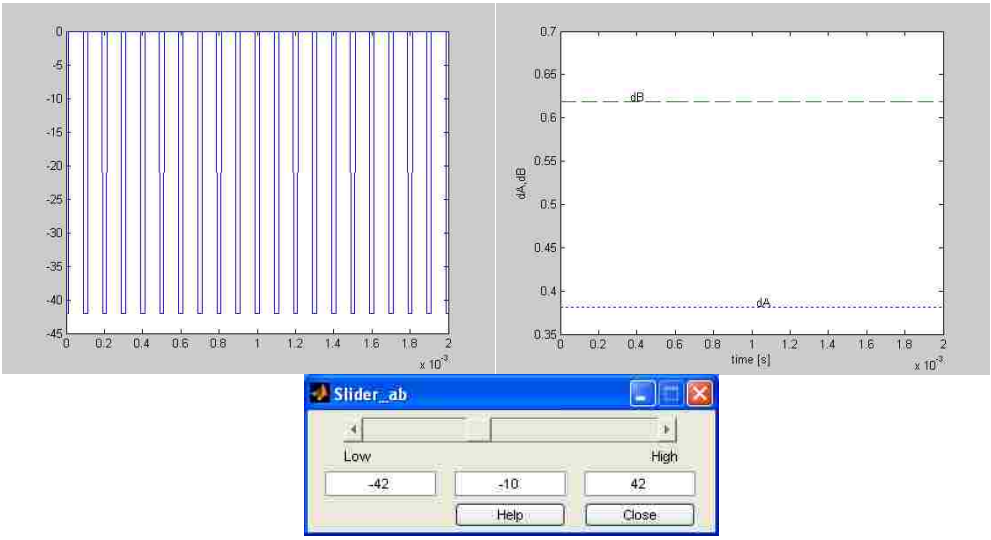

Figure 4.9 Two-pole converter model with Vout = -10V

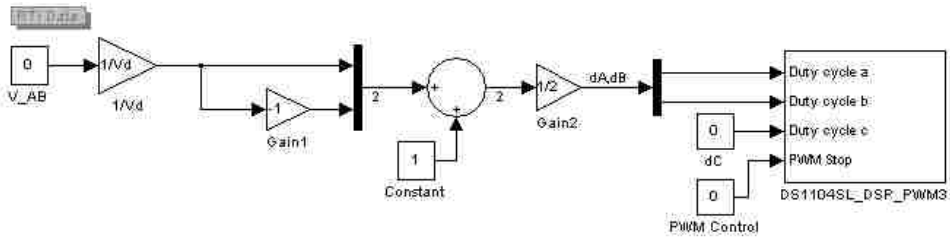

Figure 4.10 Two-pole converter model in real-time

The block **DS1104_DSP_PWM3** of the real-time in Fig.4.9 has the following block properties:

- Frequency as 10000 Hz
- Dead band as 0

The Simulation parameters are:

- Advanced block reduction is in **off** position

- Solver options:
    - Stop time: inf
    - Type: Fixed-step
    - Solver: ode1 (Euler)
    - Fixed-step size: 0.0001

The value of DC-bus voltage (Vd = 42) is assigned at the Matlab command prompt before the real-time implementation. Then the Simulink model is converted into real-time model as shown in Fig. 4.10.

4.4 Speed Control of DC Motor in Open-Loop

The real-time model of section 4.3.3 is used for no-load DC motor test. The motor terminals are connected to the phase A1 and phase B1 of the power electronics board. The **DS1104ENC_POS_C1** and **DS1104ADC_C5** blocks of **dSPACE** library are used to measure the speed and current of DC motor under control in real-time

4.4.1 Real-Time Simulink Model for No-Load DC Motor Test

The block diagram model for no-load DC motor test is shown in Fig. 4.11. In this diagram:

- The real-time model of section 4.3.3 is used as the variable voltage block to the DC motor. The constant block of section 4.3.3 named as **V_AB** is renamed to **V_motor**. This block acts as the input voltage source to the motor.
- Current Measurement Block
    - The channel 5 of the A/D converter (**ADCH 5**) on **CP 1104** is used for measuring the real-time current. The **DS1104ADC_C5** block is connected to the **Gain** block because the data has to be scaled. To filter the ripples in current waveform a transfer function block is used.

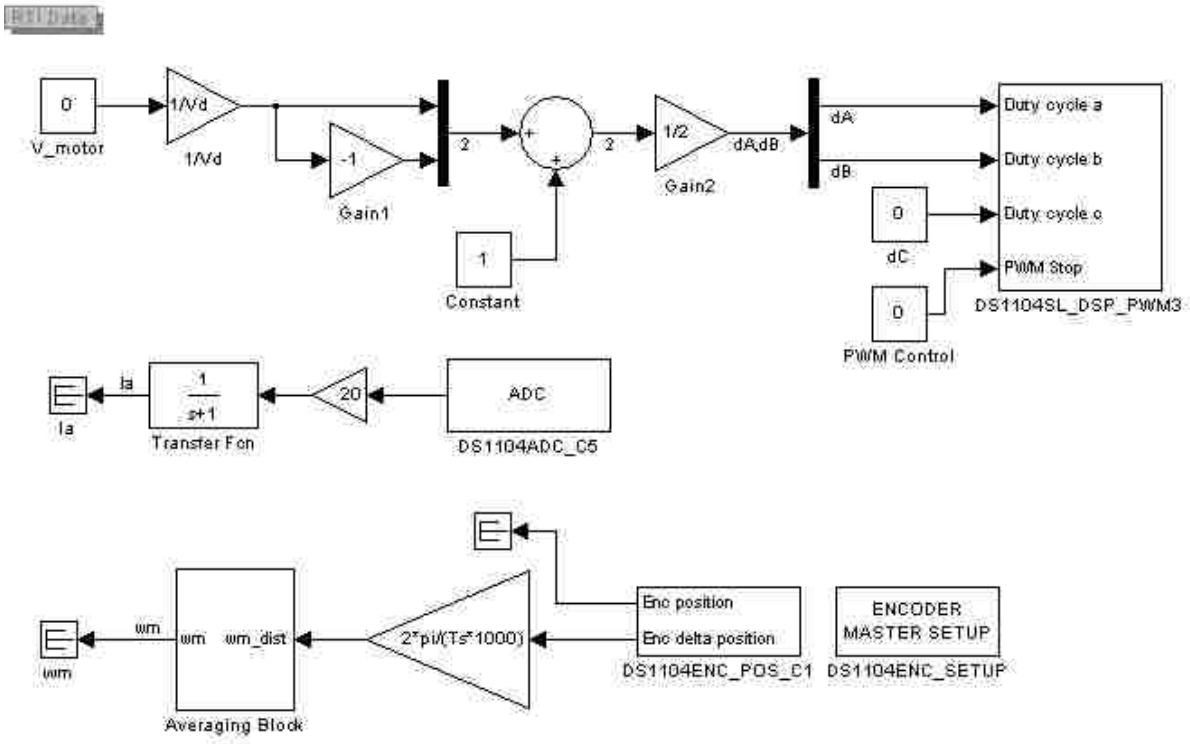

Figure 4.11 Real-time model for no-load motor test

- Speed Measurement Block
  - The **DS1104ENC_POS_C1** block gives access to the encoder in the motor, which represents the speed of the motor
  - In order to receive the radian angle the block has to be multiplied by $\frac{2\pi}{encoder_lines}$ (in our case $encoder_lines = 1000$)
  - To obtain the speed the delta position scaled has to be divided by sampling time T_s. $\omega = \frac{d\theta}{dt} = \frac{\Delta\theta}{t_{k+1} - t_k} = \frac{\Delta\theta}{T_s}$ (T_s = fixed-step time value = 0.0001)
  - At low speeds, it was observed some oscillations in average speed in order to improve the overall accuracy 11 point averaging block is constructed as shown in Fig. 4.12

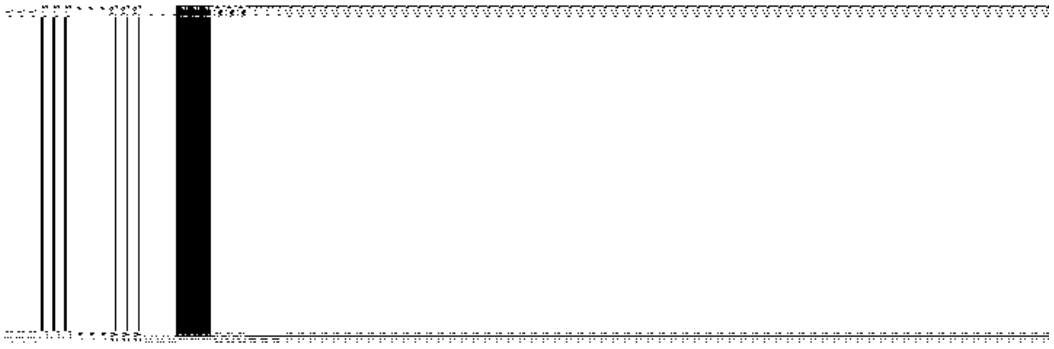

Figure 4.12 Averaging block

4.5 Results of No-Load DC Motor Test

The measurements were done at no-load for different voltages are shown in Table. 4.1. There the corresponding speed and current readings are enclosed.

Table 4.1 No-load measurement

V_motor	[V]	1.0	3.0	5.0	10.0	15.0	21.0	30.0	40.0
Speed	[rad/sec]	5.71	27.13	47.12	98.53	148.51	208.48	300.0	396.98
Current	[A]	0.32	0.34	0.36	0.41	0.43	0.45	0.48	0.52

The real-time value of armature current I_a and rotor angular speed ω_m for the supply voltage V_motor = 40V observed in the Control Desk window is shown in Fig. 4.13

The voltage vs speed curve for the no-load condition of DC machine is shown in Fig. 4.14. This characteristic can be expressed by equation:

$$y = m \cdot x + c$$

where:

slope m = 10.0423

intercept c = -2.852

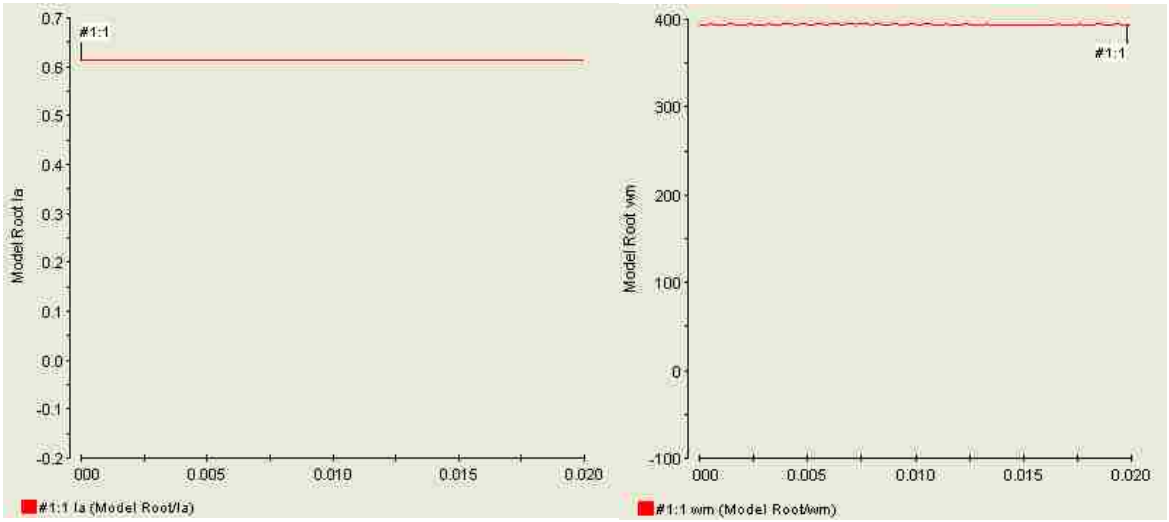

Figure 4.13 Current and speed of DC motor at V_motor = 40V displayed in Control desk

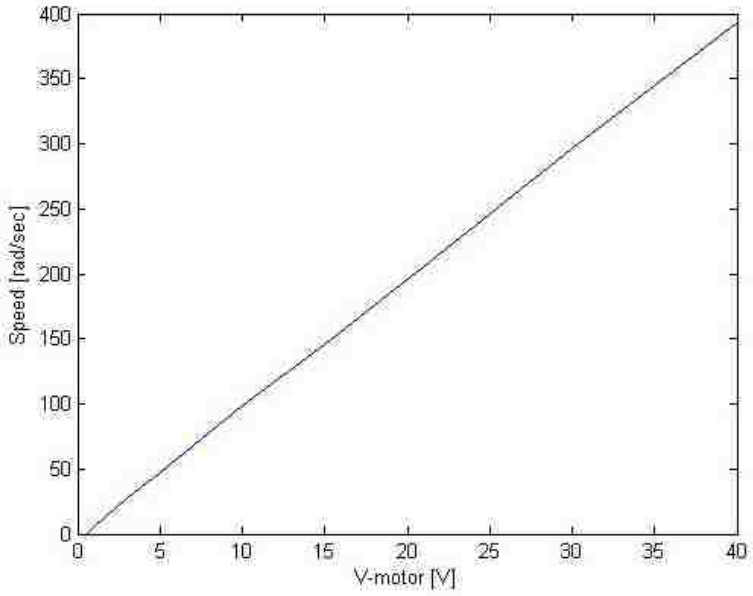

Figure 4.14 Voltage vs. speed characteristic at no-load

4.6 Conclusion

In this experiment, first, the single-pole and two-pole converter models are built and simulation results for the positive and negative values of slider gain are observed. Next, the comparator and the triangular waveform block of two-pole converter model is replaced with the **DS1104SL_DSP_PWM3** block and the converter model is implemented in real-time. Finally, real-time model for speed control of DC motor is built and the voltage-speed characteristic of DC motor is measured (see Fig. 4.14). This voltage-speed characteristic is a straight line with slope m = 10.0423 and intercept c = - 2.852.

Chapter 5

Experiment 4 – Determination of DC Motor Parameters

5.1 Introduction

In this experiment **steady-state** and **dynamic** characteristics are measured. They are, next, used to determine the motor parameters. These parameters are used to design **PI controllers** for the closed loop control of DC motor.

5.2 Steady-State Characteristics of DC Motor Drive

5.2.1 Theoretical Background

One of the main steady-state characteristics of DC motor is a speed vs torque characteristic. In each DC machine, this characteristic is linear with a constant slope. The expressions, which describe it mathematically, are as follows [6]:

$$V_M = R_a I_a + k\omega_m \tag{5.1}$$

$$T_{em} = kI_a \tag{5.2}$$

where:

ω_m – the angular rotor speed

T_{em} – electromagnetic torque developed by the motor

After re-arranging the Eqn. 5.1 the rotor speed as a function of armature current is:

$$\omega(I_a) = -\frac{R_a}{k} I_a + \frac{V_M}{k} \tag{5.3}$$

The Eqn. 5.3 can be represented by the straight line written as:

$$y = mx + c \tag{5.4}$$

where:

$$m = -\frac{R_a}{k} \tag{5.5}$$

$$c = \frac{V_M}{k} \tag{5.6}$$

The motion equation of the machine set model shown in Fig. 5.1, written for steady-state, has a form [5]:

$$T_{em} = T_L + B\omega_m + T_{fr} \tag{5.7}$$

where:

B – friction coefficient (of rotational friction)

T_{fr} – static friction torque

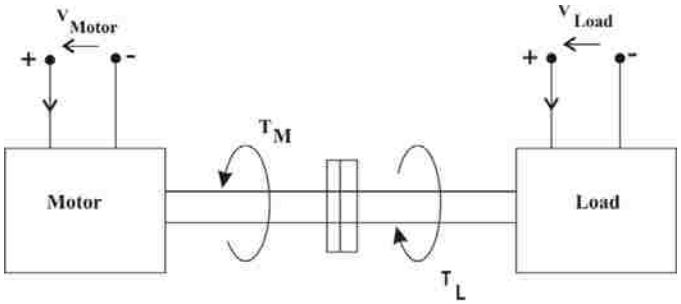

Figure 5.1 Machine set model

5.2.2 Simulink Model for Determining Steady-State Parameters

To determine the steady-state parameters the DC motor is axially coupled with the load (another DC motor). The motor under test and load are supplied from two independent PWM units, so that their voltages can be controlled independently. The Fig. 5.2 presents the real-time Simulink model for motor and load under open-loop voltage control to determine the steady-state parameters of DC motor. There are two voltage control sets. One voltage control set is for the motor and another one for the load. The output of **DS1104SL_DSP_PWM3** is fed to **Phase A1** and **Phase B1** of the Power Electronics Drives Board with the help of **37 pin DSUB** connector. Similarly the output of **DS1104SL_DSP_PWM** is fed to **Phase A2** and **Phase B2**. The blocks

DS1104ADC_C5 and **DS1104ADC_C6** are used to display the motor and load currents in Control Desk. The blocks **DS1104ENC_POS_C2** and **DS1104ENC_SETUP** are used to record to drive speed. The Fig. 5.3 shows the Control Desk Layout of real-time Simulink model for motor and load control.

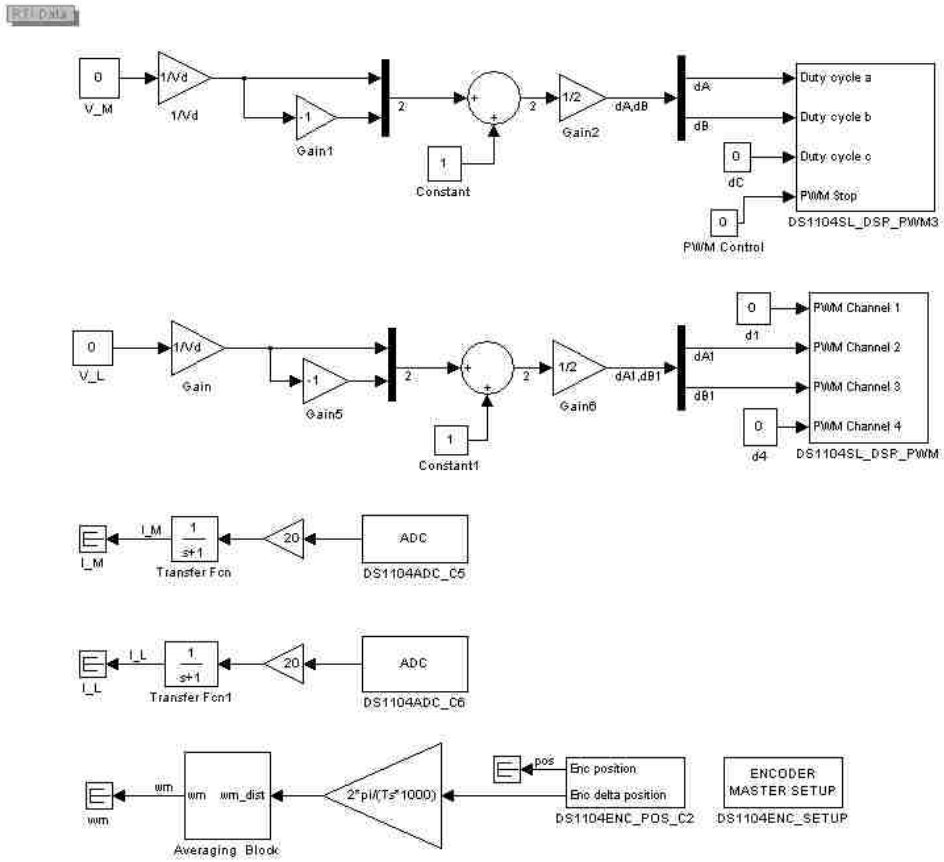

Figure 5.2 Real-time Simulink model for motor and load control

5.2.3 Determination of Steady-State Parameters

– Estimation of motor constant k:

By supplying the motor with the rated **armature voltage**, keeping the load in the active region, such that the motor current $\boldsymbol{I_a}$ is **zero** the speed is recorded and $\boldsymbol{k}$ is calculated as:

$$k = \frac{V_{a_rated}}{\omega_m} \tag{5.8}$$

for $V_{a_rated} = 40V$ the speed is recoded as $\omega_m = 372\ rad/s$. By substituting this values in Eqn. 5.8: $k = 0.107\ [V/rad/s]$

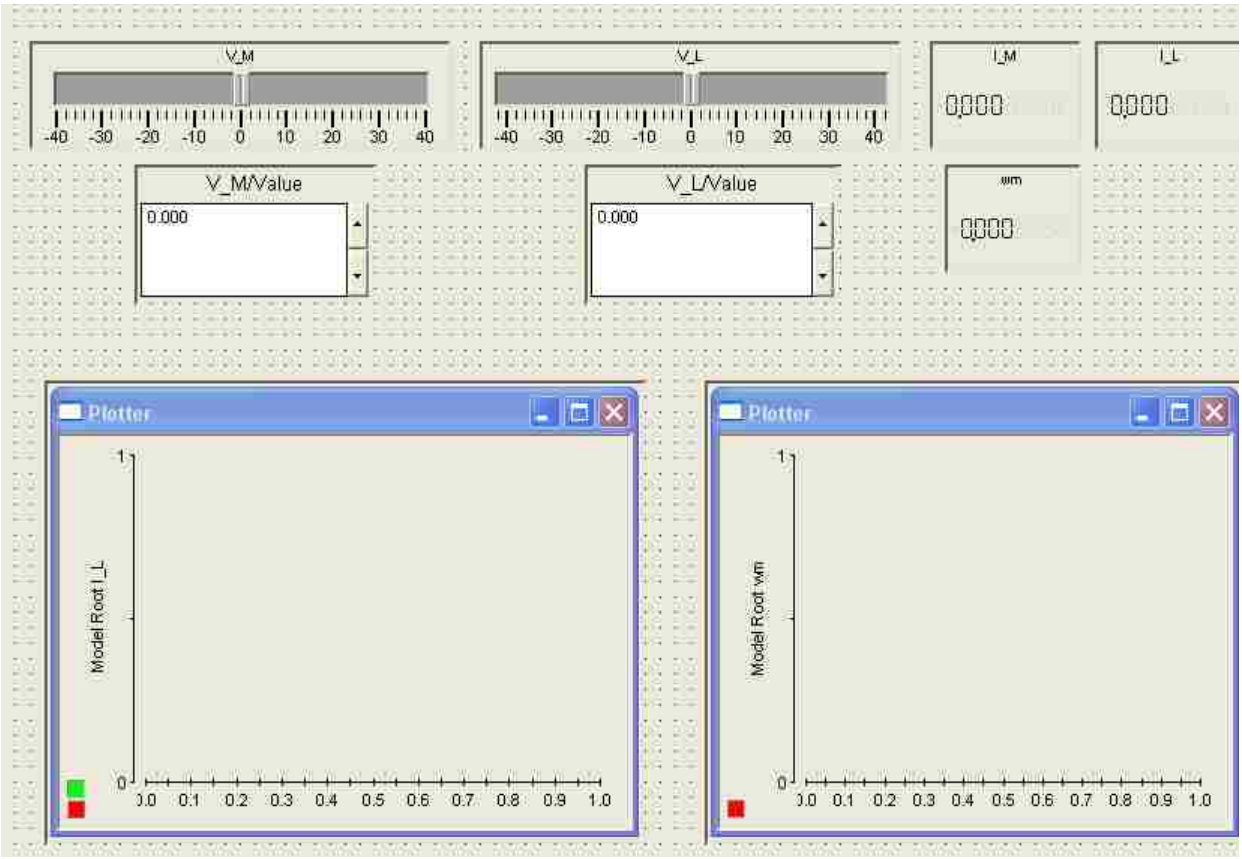

Figure 5.3 Control Desk layout of real-time Simulink model for motor and load control

– Torque-speed characteristics:

For different motor voltage constant values say: [5 10 20 30 40] V the load voltage is adjusted such that, the motor current takes the values as [0 1 2 3 4 5] A. At each voltage level the speed, the load current, and the load voltage are recorded. The list of recorded values for different voltage levels is presented in Table. 5.1. The torque column is obtained by multiplying motor current $\boldsymbol{I_M}$ with motor constant $\boldsymbol{k}$. Using the Matlab the slope (m) and intercept (c) of the recorded values are determined.

Table 5.1 Steady–state experimental data

V_M [V]	V_L [V]	I_M [A]	I_L [A]	ω_m [rad/s]	T_{em} [N·m]
5	-6.5	0	-1.02	51.4	0
	-3.8	1	0.03	38.5	0.107
	-1.4	2	1.05	28.5	0.215
	0.35	3	1.97	19.9	0.322
	2.1	4	2.95	11.4	0.430
	3.8	5	3.87	2.8	0.537
10	-12.0	0	-1.11	101.3	0
	-9.0	1	0	81.5	0.107
	-6.8	2	0.92	75	0.215
	-4.8	3	1.85	69.5	0.322
	-3.1	4	2.85	59.9	0.430
	-1.2	5	3.78	51.4	0.537
20	-22.8	0	-1.42	204.6	0
	-19.9	1	-0.34	185.0	0.107
	-17.5	2	0.54	168.6	0.215
	-15.6	3	1.43	157.0	0.322
	-13.5	4	2.46	141.3	0.430
	-11.3	5	3.53	125.0	0.537
30	-33.1	0	-1.23	292.7	0
	-30.3	1	-0.24	278.3	0.107
	-27.3	2	0.74	265.0	0.215
	-25.2	3	1.55	257	0.322
	-23.1	4	2.45	242	0.430
	-21.0	5	3.33	228.7	0.537
40	-41.5	0	-1.32	372.0	0
	-38.6	1	-0.31	355.4	0.107
	-35.5	2	0.62	345.5	0.215
	-33.1	3	1.52	334.7	0.322
	-30.5	4	2.47	315.5	0.430
	-28.3	5	3.3	297.8	0.537

The speed-torque characteristics drawn for the motor using the data presented in Table. 5.1 are shown in Fig. 5.4. Theoretically these characteristics should be the straight lines described by the function (Eqn. 5.4):

$$\omega_m(I_a) = mI_a + c \tag{5.9}$$

Practically, these characteristics are not straight lines.

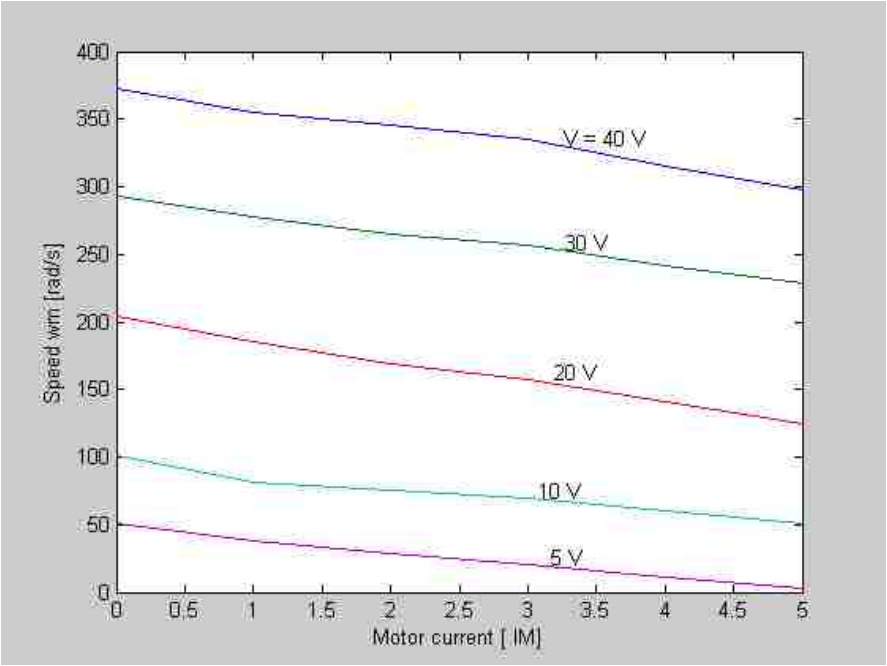

Figure 5.4 Speed vs. armature current characteristics for motor voltage supplied by different voltages

The slope **m** and the intercept **c** of the characteristics for each constant voltage level are determined using Matlab m-file and are listed in Table. 5.2. The values of $\boldsymbol{k}$ and $\boldsymbol{R_a}$ are calculated as:

$$k_i = \frac{V_{a_i}}{c_i} \tag{5.10}$$

where: i = 1, 2, 3, 4, 5 is the subsequent number voltage level considered in Table. 5.1

$$R_{a_i} = -k_i \cdot m_i \tag{5.11}$$

The average value of $\boldsymbol{k}, \boldsymbol{m}$ and $\boldsymbol{R_a}$ is calculated as:

$$k = \frac{\sum_{i=1}^{n} k_i}{n}, \qquad m = \frac{\sum_{i=1}^{n} m_i}{n}, \qquad R_a = \frac{\sum_{i=1}^{n} R_{a_i}}{n} \tag{5.12}$$

where $n = 5$

Table 5.2 Steady-state parameters

V_{a_i} [V]	m_i (slope)	c_i (intercept)	k_i [V/(rad/s)]	R_{a_i} [Ω]
40	-14.32	372.63	0.107	1.43
30	-12.48	291.82	0.102	1.24
20	-15.44	202.20	0.09	1.54
10	-9.13	95.94	0.104	0.90
5	-9.15	49.19	0.101	0.95

The average values of motor parameters are in Table 5.3.

Table 5.3 Average values of motor parameters

m (slope)	c (intercept)	k $[V/(rad/s)]$	R_a [Ω]
-12.104	202.356	0.1	1.212

– Determination of mechanical model parameters

The mechanical model parameters B and T_{fr} are determined by running the motor under **no-load** condition.

The Eqn. 5.7 under no-load condition can be written as:

$$T_{em} = B\omega_m + T_{fr} \tag{5.13}$$

For different motor voltages the values of speed and armature current of motor are recorded and listed in Table. 5.4.

Table 5.4 Steady-state friction model characteristics

V_M [V]	I_M [A]	ω_m [rad/s]	T_{em} [N·m]
1.0	0.32	5.71	0.03424
3.0	0.34	27.13	0.03638
5.0	0.36	47.12	0.03852
10.0	0.41	98.53	0.04387
15.0	0.43	148.51	0.04601
21.0	0.45	208.48	0.04815
30.0	0.48	300.0	0.05136
40.0	0.52	396.98	0.05564

The torque-speed characteristic of the steady-state frictional model is shown in Fig. 5.5

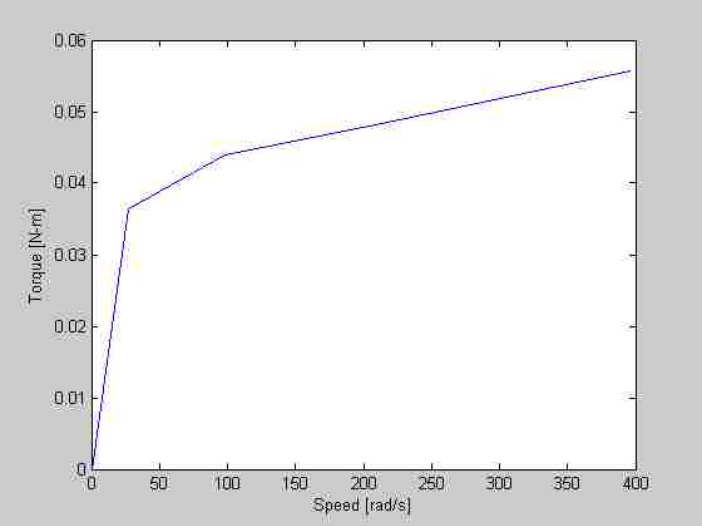

Figure 5.5 Torque-speed characteristic of steady state friction model

The mechanical model parameters B and Tfr (see Eqn. 5.13) are calculated using data of Table 5.4 are shown in Table 5.5.

Table 5.5 Mechanical steady state parameters

m = B [N.m/(rad/s)]	c = T_{fr} [N.m]
0.0001	0.0362

5.3 Dynamic Characteristics of DC Motor Drive

5.3.1 Theoretical Background

The dynamics of DC machine can be specified as **electrical** (transients) and **mechanical** dynamics. From the dynamic characteristics of DC motor, the armature inductance (L_a) and moment of inertia (J) can be determined.

The dynamic equations of a DC motor are:

$$V_a = R_a i_a + k\omega_m + L_a \frac{di_a}{dt} \tag{5.14}$$

$$T_{em} = T_L + T_{fr} + B\omega_m + J \frac{d\omega_m}{dt} \tag{5.15}$$

In Eqn. (5.14) and (5.15), the two state variables: armature current (i_a) and angular speed (ω_m) are not independent. So both: armature inductance (L_a) and moment of inertia (J) can vary if any one of the state variables is changed.

– Determination of armature inductance (L_a):

The armature inductance of DC motor is calculated by keeping the motor in **standstill** ($\omega_m = 0$). Then Eqn. 5.14 can be written as:

$$V_a = R_a i_a + L_a \frac{di_a}{dt} \tag{5.16}$$

By solving the Eqn. 5.16 with respect to the current we obtain:

$$i_a(t) = \frac{V_a}{R_a}\left(1 - e^{-\frac{t}{\tau_a}}\right) \tag{5.17}$$

where:

$$\tau_a = \frac{L_a}{R_a}$$

The curve that represents Eqn. 5.17 is shown in Fig. 5.6. The slope of this exponential curve measured at $t = 0$, is depended on the value of inductance (L_a) and is given as:

$$\left.\frac{di_a}{dt}\right|_{t=0} = \frac{V_a}{L_a} \tag{5.18}$$

By knowing the slope at a given voltage, inductance can be determined as follows:

$$L_a = \frac{V_a}{slope} \tag{5.19}$$

where:

$$slope = \frac{I_a}{\Delta t} \tag{5.20}$$

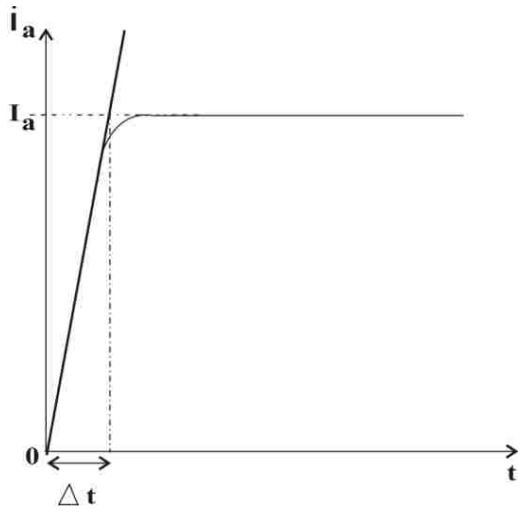

Figure 5.6 Current response at standstill ($\omega_m = 0$)

– Determination of moment of inertia (J):

In order to determine the moment of inertia the armature current (i_a), the load torque (T_L) and motor torque (T_{em}) must be zero. In order to achieve this the motor should rotate with **no-load speed** (ω_0) and has to maintain zero armature current ($i_a = 0$). Then the whole system has to shutdown at $t = 0$. This implies the load torque (T_L) and motor torque (T_{em}) becomes zero. For these conditions the dynamic Eqn. 5.15 can be written as:

$$0 = T_{fr} + B\omega_m + J\frac{d\omega_m}{dt} \tag{5.21}$$

When the system is shutdown the speed decreases exponentially in time and is given as:

$$\omega_m(t) = \left(\omega_0 + \frac{T_{fr}}{B}\right) e^{-\frac{B}{J}t} - \frac{T_{fr}}{B} \tag{5.22}$$

The static frictional torque T_{fr} depends on speed. So it should become zero once the speed reaches zero, otherwise it will become an active torque and drive the motor into the fourth quadrant.

Rearranging Eqn. 5.22 we obtain:

$$\Omega = \Omega_0 e^{-\frac{B}{J}t} \tag{5.23}$$

where:

$$\Omega = \omega_m(t) + \frac{T_{fr}}{B}$$

$$\Omega_0 = \omega_0 + \frac{T_{fr}}{B}$$

From Eqn. 5.23 the moment of inertia depends on the slope of curve (see Fig. 4.7) at $t = 0$:

$$\left.\frac{d\Omega}{dt}\right|_{t=0} = -\Omega_0 \frac{\mathrm{B}}{\mathrm{J}} \tag{5.24}$$

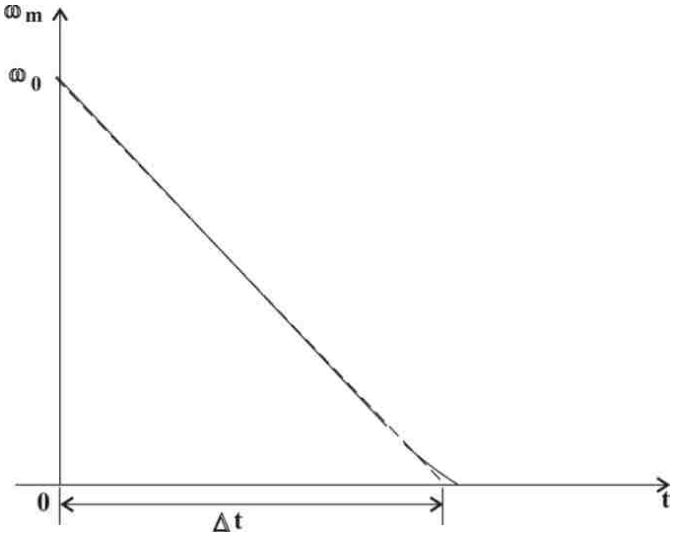

Figure 5.7 Speed response when the system is made to shut down

Since the slope at t=0 is equal to $\left(-\frac{\omega_o}{\Delta t}\right)$, the moment of inertia is calculated as:

$$J = -\omega_0 \frac{B}{slope|_{t=0}} \tag{5.25}$$

where:

$$slope|_{t=0} = -\frac{\omega_0}{\Delta t}$$

5.3.2 Simulink Model for Dynamic Parameter Determination

To determine the dynamic parameters of a DC motor, it should be axially coupled with another DC motor (load). These two DC motors (i.e. DC motor under test and load) are supplied with two independent PWM converters. The DC motor under test is controlled in **open-loop** with variable voltage and the load is **current** controlled.

The Simulink model of section 5.2.2 (Fig. 5.2) is also used in this section in modified version shown in Fig. 5.8. Determination of the electrical and dynamic parameters requires either a positive or negative step change in supply voltage. This is achieved by the reset block shown in Fig. 5.8. In order to determine the moment of inertia the armature current of DC motor under test must be zero and the motor should not enter into the regenerative braking mode with negative torque. This is achieved by the **SHUTDOWN** signal on the Power Electronics drive board.

The **DS1104SL_DSP_BIT_OUT_C11** and **DS1104SL_DSP_BIT_OUT_C12** of dSPACE library are added to achieve the open circuit of armatures from the supply, so that the motor will not enter into regenerative braking mode with negative torque.

The Control Desk layout for dynamic parameters determination is shown in Fig. 5.9.

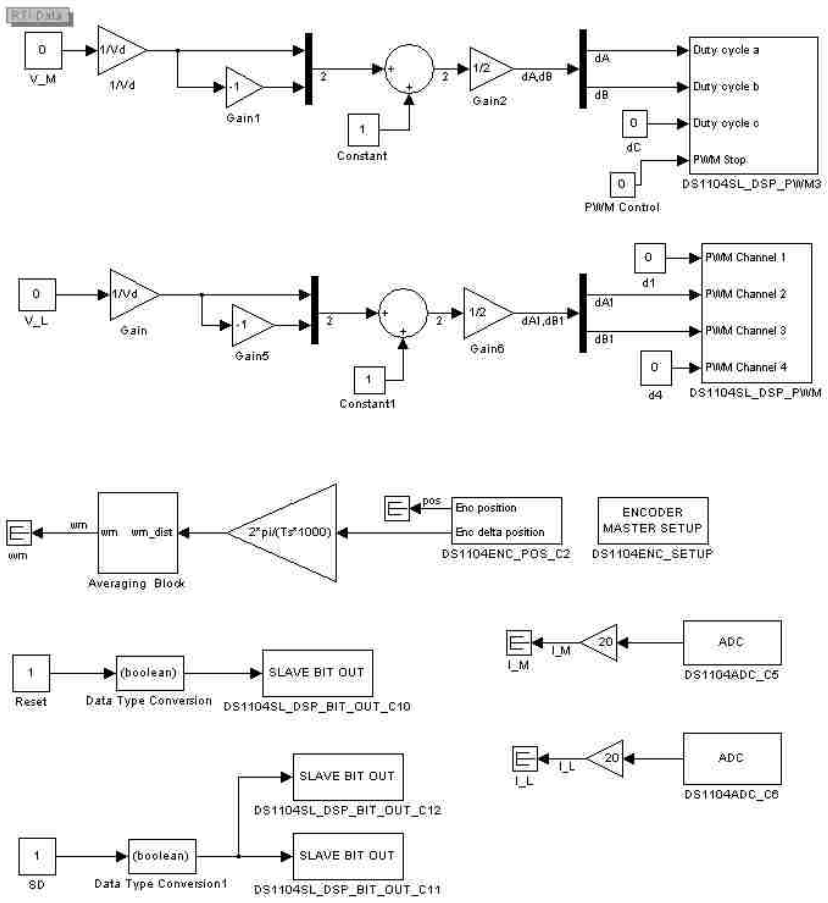

Figure 5.8 Simulink model for dynamic parameters determination

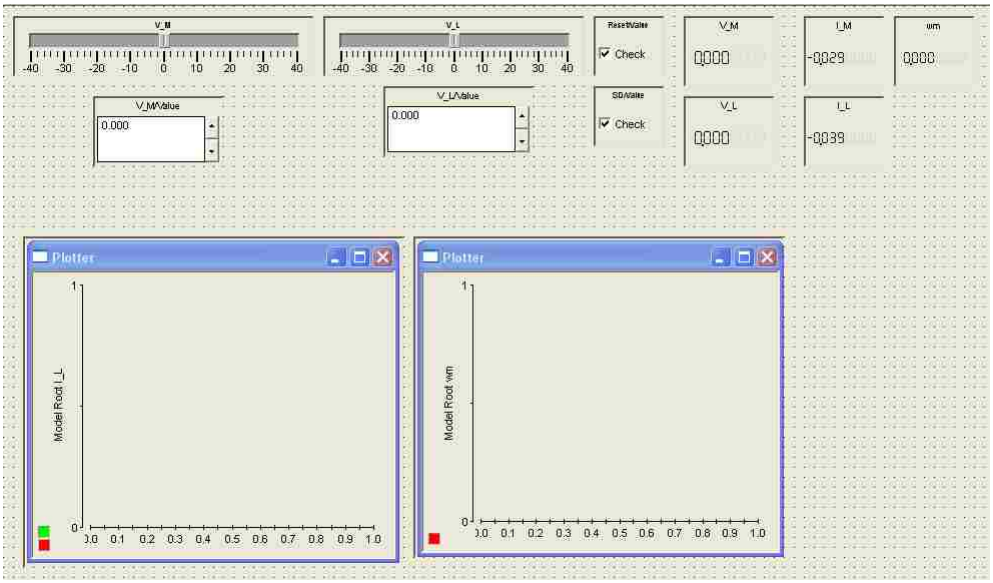

Figure 5.9 Control desk layout for dynamic parameters determination

5.3.3 Inductance Determination

In order to determine the **inductance** of DC motor under test the rotor of coupled drive is blocked (the speed of the drive $\omega_m = 0$). Now, a step in voltage of V_M = 3V is applied. The current increased exponentially and reached the steady state value. The measured characteristic is shown in Fig. 5.10. The slope of the exponential curve is obtained from the following Matlab program (the curve fitting algorithm):

%calculation of DC motor inductance and resistance using a curve fitting algorithm [2]

```
global Plothandle t y y0;
load ind;
t=ind.X.Data;
y=ind.Y(:,2).Data;
nmax=length(y);
y0=mean(y((nmax-1)/2:nmax));
cla reset;
axis([0 .2 0 3.5])
hold on;
plot(t,y,'r','Erasemode','none');
title('Armature current response'); ylabel('current [A]'),xlabel('time [s]');
hold on;
Plothandle=plot(t,y,'Erasemode','x');
lam0=[100];
lamda=fminsearch('fitraz',lam0);
hold off;
```

```
V=3;

i0=y0

Ra=V/i0

La=Ra/lamda
```

%curve fitting algorithm [2]

```
function err=fitcur(lambda)

global Plothandle t y y0;

A=zeros(length(t),length(lambda));

for j=1:length(lambda)

    A(:,j)=exp(-lambda(j)*t)';

end

c=A\(y-y0)';

z=A*c;

set(Plothandle,'ydata',z+y0);

drawnow;

err=norm(z-(y-y0)');
```

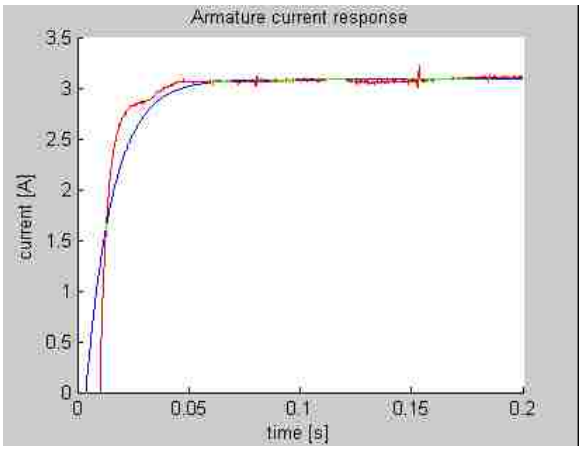

Figure 5.10 Armature current response for a step changed voltage V_M = 3V

The inductance calculated for the given motor is:

$$L_a = 0.0118\ H$$

5.3.4 Determination of Moment of Inertia

To determine the moment of inertia the armature voltage is increased to 40V and by supplying the negative voltage to the load the armature current is maintained zero. The speed at this operating point was **372 rad/s**. At this point the system is made to shut down by unchecking the shut down button in Control Desk. After the complete shutdown of system the speed of the motor is gradually falling down. This is shown in Fig. 5.11. The slope of the curve is determined using the following Matlab program:

```
%inertia determination [2]
global Plothandle t y y0;
load jeq;
t=jeq.X.Data;
y=jeq.Y(:,3).Data;
B=0.0000595;
Tf=0.0421;
y0=-Tf/B;
cla reset;
axis([0 2 0 450]);
hold on;
plot(t,y,'r','EraseMode','none');
title('Speed Response');
hold on;
```

```
Plothandle=plot(t,y,'EraseMode','x');

lam0=[1];

lamda=fminsearch('fitraz',lam0);

hold off;

wfin=y0

J=B/lamda
```

The moment of inertia of DC motor is calculated as according to the Eqn. 5.15 and is equal:

$$\boldsymbol{J = 2.4371e-004\ [kg \cdot m^2]}$$

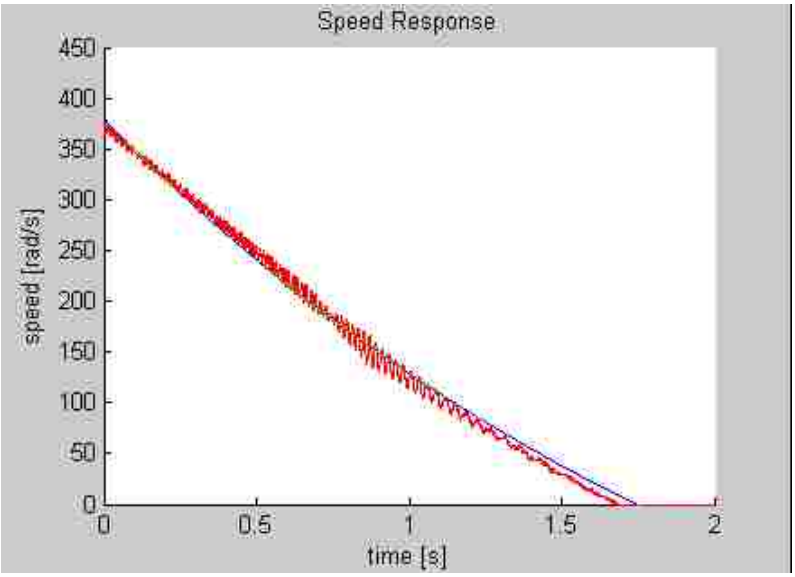

Figure 5.11 Speed of the DC motor when the system is made to shutdown

5.4 Conclusion

In this experiment DC motor parameters were determined by doing the measurement in steady-state and dynamic conditions. In no-load operation the motor constant $\boldsymbol{k}$ was determined by supplying the motor with rated armature voltage V_M = 40V and controlling the load in active region such that armature current $\boldsymbol{I_a}$ was maintained zero.

A set of measurements were taken for different supply voltages to determine the speed vs. torque characteristics in steady-state. Next, the DC motor was tested without load to determine the friction model parameters.

The measurements were done in transients with the rotor blocked and in dynamic conditions to determine the inductance and moment of inertia.

The DC motor parameters determined are:

$R_a = 0.9725\ \Omega$

$L_a = 0.0118$ H

$k = 0.107\ [V/rad/s]$

$B = 0.0001\ [N \cdot m/(rad/s)]$

$T_{fr} = 0.0362\ [N \cdot m]$

$J = 2.4371e-004\ kg \cdot m^2$

These parameters will be used in the next experiment for close-loop control.

Chapter 6

Experiment 5 – DC Motor Control

6.1 Introduction

In this experiment the PI controllers for current and speed are designed using the DC motor parameters determined in the previous experiment (Determination of DC motor parameters). The designed controllers are tested on the simulation model of the DC motor. When the parameters of the controllers are tuned properly the model of the DC motor is replaced with the real DC motor. Next, the real DC motor is controlled (using the current and speed controllers) with the help of dSPACE board.

6.2 Simulink Model of DC Motor with Current and Speed Controller

The armature current (I_a) and rotor speed (ω_m) of a DC motor written in Laplace Transform can be calculated as [1]:

$$I_a(s) = \frac{V_a(s) - E_a(s)}{R_a + sL_a} \tag{6.1}$$

$$\omega_m(s) = \frac{T_{em}(s) - T_L(s)}{sJ_{eq}} \tag{6.2}$$

where:

$$E_a(s) = k_e \omega_m(s) \tag{6.3}$$

$$T_{em}(s) = k_t I_a(s) \tag{6.4}$$

$$k_e = k_t = k \tag{6.5}$$

The above equations will be implemented in Simulink.

– DC motor Simulink model

The Simulink model of DC motor shown in Fig. 6.1 consists of i**ntegrators** instead of transfer functions to set initial conditions for current and speed state variables. The parameter values for the Simulink model (obtained from the previous experiment DC motor characterization) are:

$R_a = 0.9725\ \Omega$

$L_a = 0.0118$ H

$k_e = k_t = k = 0.107\ [V/rad/s]$

$B = 0.0001\ [N \cdot m/(rad/s)]$

$J = 2.4371e-004\ kg \cdot m^2$

The model is next converted into the sub-system.

Figure 6.1 Simulink model of DC motor

– PI current controller [4]

The parameters of current controller $(K_{i_i}\ and\ K_{p_i})$ are determined from the following Eqns. 6.6 and 6.7 [4]:

$$K_{i_i} = \frac{\omega_{c_i} R_a}{K_{pwm}} \tag{6.6}$$

$$K_{p_i} = K_{i_i}\frac{L_a}{R_a} \tag{6.7}$$

For the values of motor parameters R_a and L_a mentioned earlier and assuming that:

$K_{pwm} = 42$

$\omega_{c_i} = 2\pi f_{c_i} = 1500\ rad/s$ (for the cross over frequency $f_{c_i} = 238\ Hz$)

the controller gains are equal:

$K_{i_i} = 34.7$

$K_{p_i} = 0.42$

The Simulink model of **PI current controller** is shown in Fig. 6.2. The **upper** and **lower** saturation limits of the **Integrator** and **Saturation** blocks were set to **+1** and **-1** values respectively.

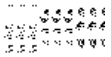

Figure 6.2 PI current controller

The Simulink model of DC motor with the current controller is shown in Fig. 6.3. In this model **Ia_ref = 1** and **Kpwm = 42**.

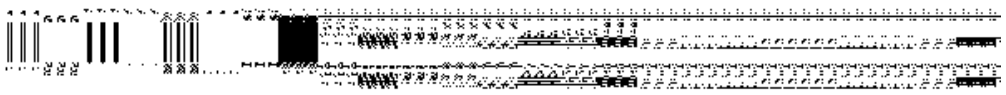

Figure 6.3 Simulink model of DC motor with current controller

The results obtained from simulation are shown in Figs. 6.4 and 6.5 in form of current and speed waveforms. As one can see the actual current reaches the reference value in a very short time. The motor speed is increasing linearly since there is no load torque and the friction of the motor is negligible.

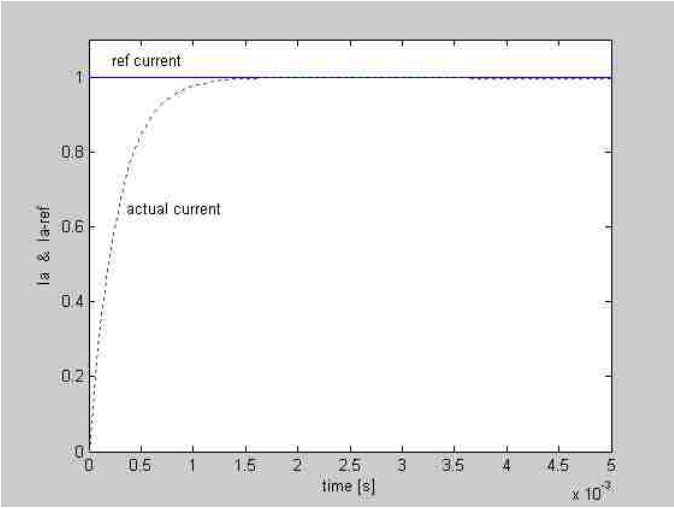

Figure 6.4 Current waveform for Ia_ref = 1 A

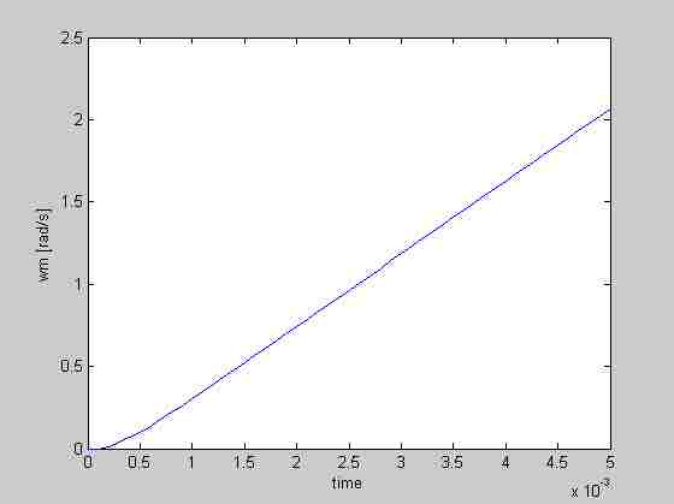

Figure 6.5 Speed waveform for Ia_ref = 1 A

– PI speed controller

The parameters of the PI speed controller were determined from the following equations [4]:

$$-\frac{K_{i_\omega} \cdot k_t}{J \cdot \left(\omega_{c_\omega}\right)^2} = \cos\left(\emptyset_{pm} - 180^{\circ}\right) \tag{6.8}$$

$$-\frac{K_{p_\omega} \cdot k_t}{J \cdot \omega_{c_\omega}} = \sin\left(\emptyset_{pm} - 180^{\circ}\right) \tag{6.9}$$

For the crossover frequency $\omega_{c_\omega} = 2\pi f_{c_\omega} = 2\pi\ rad/s$ ($f_{c_\omega} = 1\ Hz$) and the phase margin $\emptyset_{pm} = 60^{\circ}$ the gains of PI speed controller have the values:

$$K_{i_\omega} = 0.04 \tag{6.10}$$

$$K_{p_\omega} = 0.01 \tag{6.11}$$

In the PI speed controller shown in Fig. 6.6 the **upper** and **lower** saturation limits of the **Integrator** and **Saturation** block were set to **+5** and **-5** values respectively to limit the current during transients.

The Simulink model of DC motor with cascade control (i.e. with speed and current controller) is shown in Figs. 6.7.a and 6.7.b. The reference speed is provided to the speed controller using the **Step** block or **Constant** block. The Step block has the following parameters:

- Step time – 2 s
- Initial value – 200 rad/s
- Final value – 420 rad/s

The value of the **Constant** block is **1**.

The load torque is provided to the DC machine by the **Constant** block with the constant value of **0 N·m** or by **Step** block with the following parameters:

- Step time – 4 s
- Initial value – 0.1 N·m
- Final value – 0.4 N·m

The simulation of speed-control loop for DC motor was done for two cases:

- with the constant reference speed and step-changing load torque (Fig. 6.7.a)
- with the step-changing reference speed and constant load torque (Fig. 6.7.b)

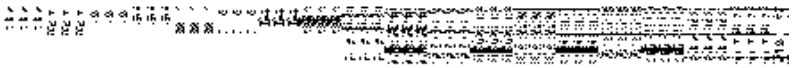

Figure 6.6 PI speed controller

Figure 6.7.a Simulink model of DC motor with cascade control for step changing load

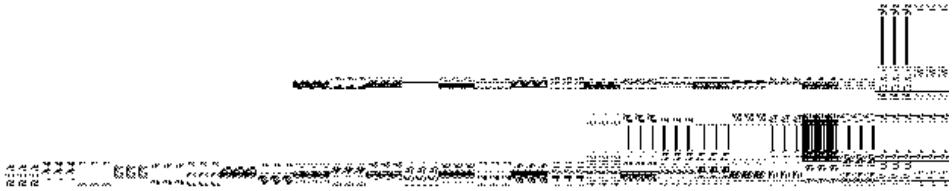

Figure 6.7.b Simulink model of DC motor with cascade control for constant load

The current and speed waveforms of the DC motor with cascade control are shown in Figs. 6.8 through 6.11. In Figs. 6.8 and 6.10 the actual current follows the reference current. This is due to the current controller. The same is with the motor speed (Figs. 6.9 and 6.11).

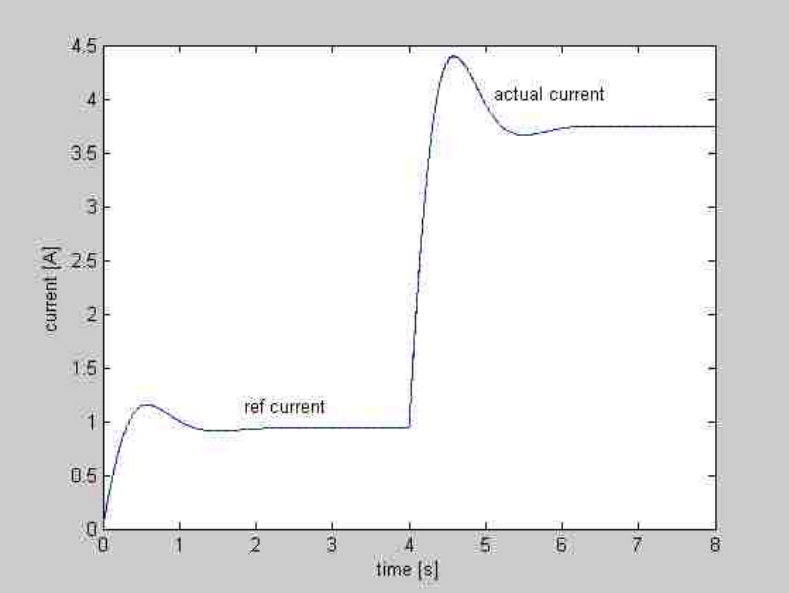

Figure 6.8 Current waveforms for step change in load

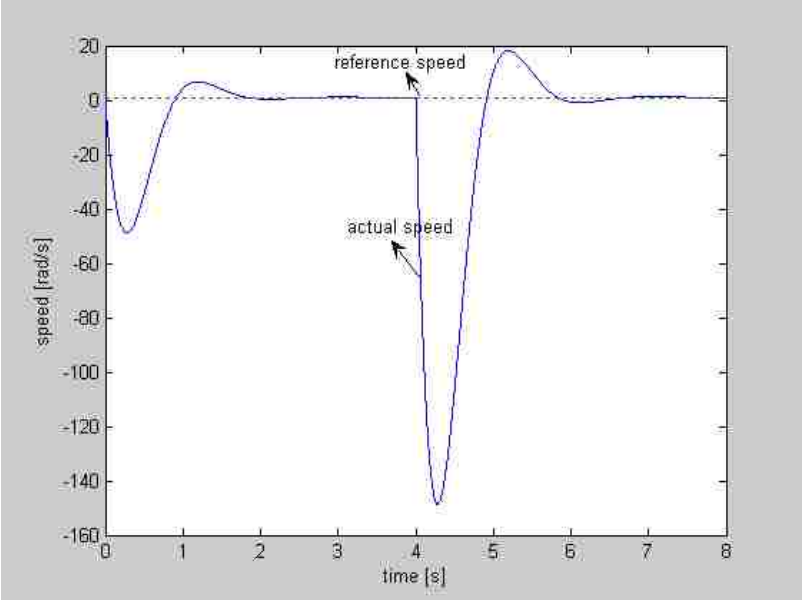

Figure 6.9 Speed waveforms for step change in load

When the reference speed is kept constant the motor actual speed returns to the previous value after the disturbance is introduced to the system by the step-change in load torque (see Fig. 6.9). When the reference speed has changed at constant zero load torque the actual motor speed changes too to the final reference speed value with the initial overshoot (see Fig. 6.11).

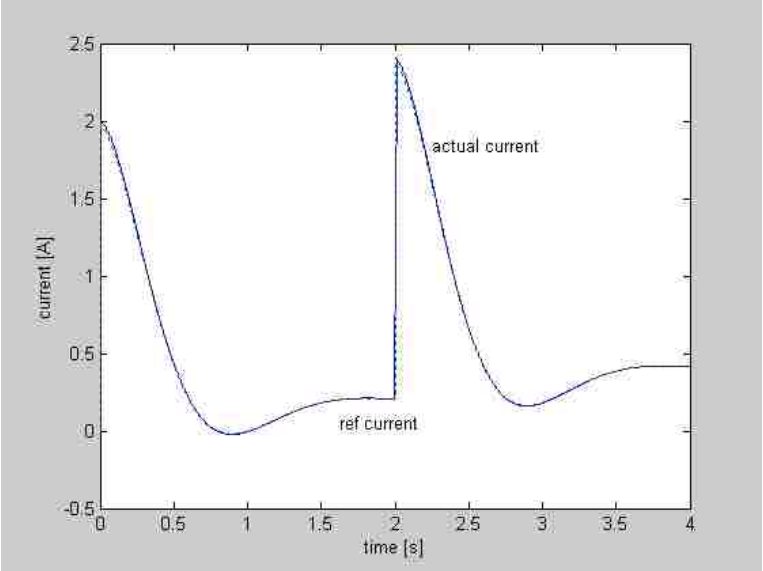

Figure 6.10 Current waveforms for step changing speed at constant load

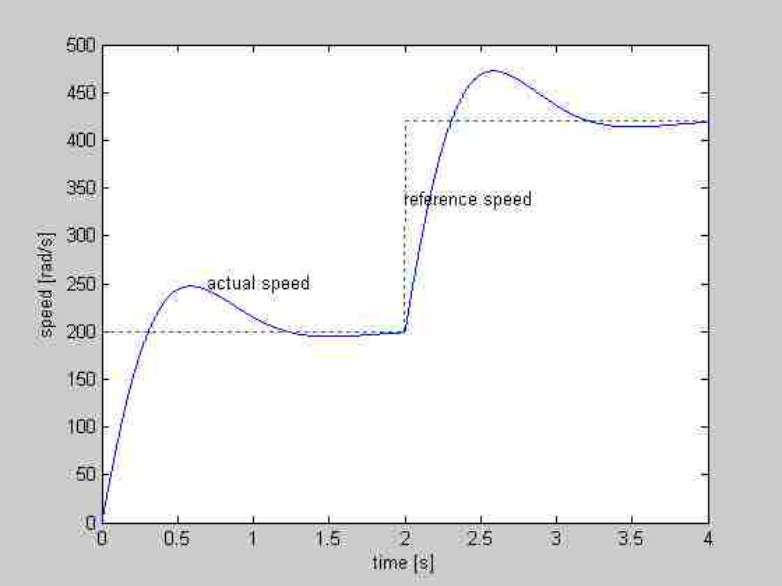

Figure 6.11 Speed waveforms for step changing speed at constant load

6.3 Real-Time Implementation of Feed–Back Control of DC Motor

The real-time Simulink model of cascade control of DC motor is shown in Fig. 6.12. In real-time the Simulink model of DC motor is replaced with the real motor and the Kpwm block is replaced by power converter with 42 V DC supply. The **Integrators** of current and speed controllers (Figs. 6.13.a and 6.13.b) are supplied with the external reset as shown in Fig. 6.12 to start up correctly in the real-time environment. The **Step** block has initial value of 50 [rad/s] and final value of 100 [rad/s] with step time of 3 s.

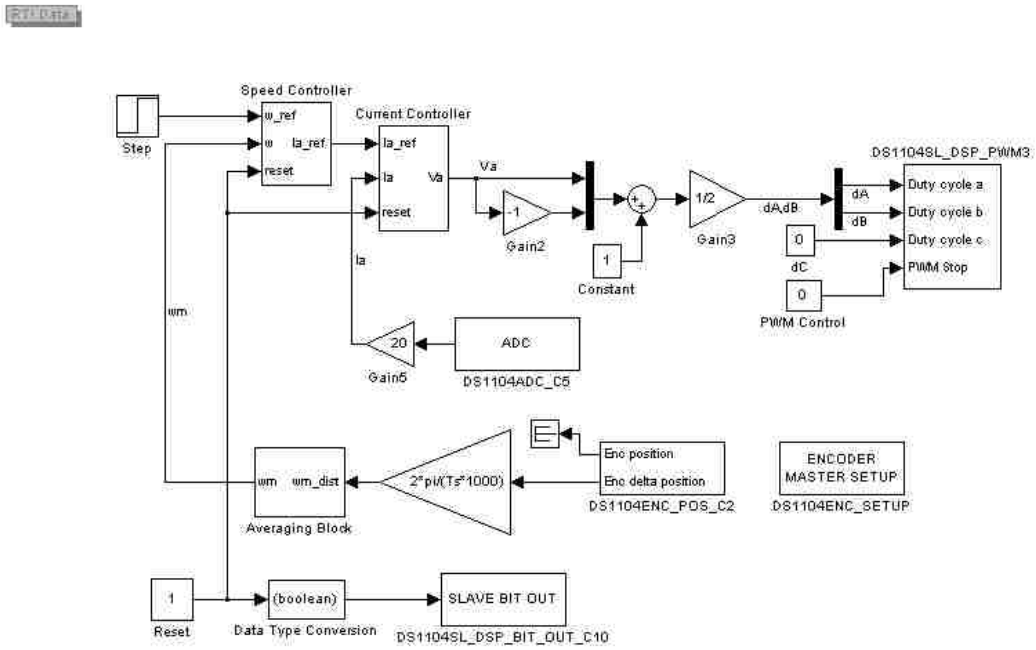

Figure 6.12 Real-time Simulink model of cascade control of DC motor

The Simulink model is implemented in real-time and the current and speed waveforms for step changing speed in real time are shown in Fig. 6.14.

6.4 Conclusion

In this experiment the current and speed controllers were designed for the Simulink DC motor model. After proper tuning of controllers the cascade control of DC motor is implemented in real-time.

The results obtained from simulation and from the measurements show that both, the actual current and speed waveforms follow the reference values with a small overshoot.

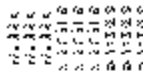

Figure 6.13.a Current controller with external reset

Figure 6.13.b Speed controller with external reset

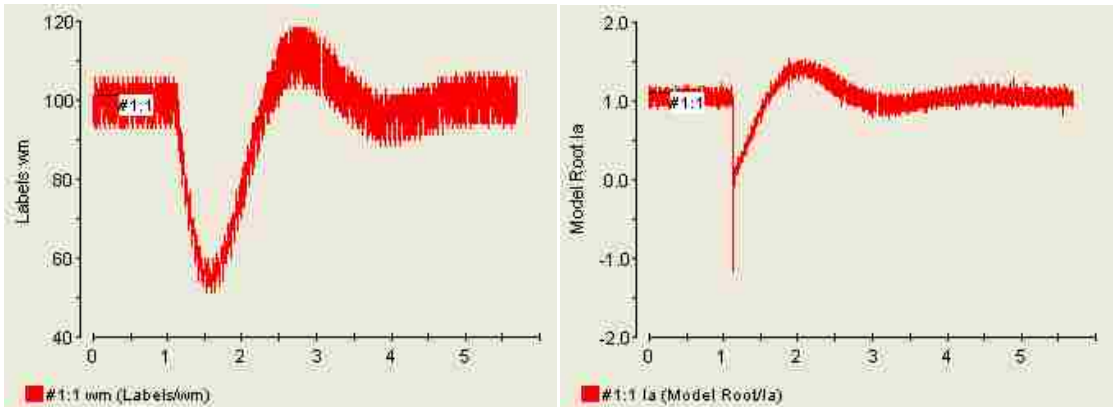

Figure 6.14 Speed and current waveforms for step change in speed

Chapter 7

Experiment 6 – Four-Quadrant Operation of DC Motor

7.1 Introduction

In this experiment, the DC motor is performed in **four-quadrant** operation. This operation is achieved by giving an alternating reference speed command to the DC motor. The PI controllers (for speed and current) designed in the previous experiment are used in the motor operation with alternating reference speed.

7.2 Simulink Model of Four-Quadrant Operation of DC Motor

The Fig. 7.1 presents the Simulink model for four-quadrant operation of DC motor. This model uses **Wref_4quad** block (Repeating Sequence block from Simulink Sources library) to generate the alternating reference speed command (**500 r/min** to **-500 r/min** with a constant ramp). The parameters of this block are as follows:

- Time values – [0 5 15 20 25 35 40]
- Output values – [0 500 500 0 -500 -500 0]

The block diagram and the gain values of the controllers (for speed and current) determined in the previous experiment are used to perform the four-quadrant operation.

The actual current with respect to reference current and V_motor is shown in Fig. 7.2.a. The actual speed of the DC motor with respect to the reference speed (wref_4quad) is shown in Fig. 7.2.b.

The actual current and speed follow exactly the reference speed and current with due to their controllers.

Figure 7.1 Simulink model for four-quadrant operation of DC motor

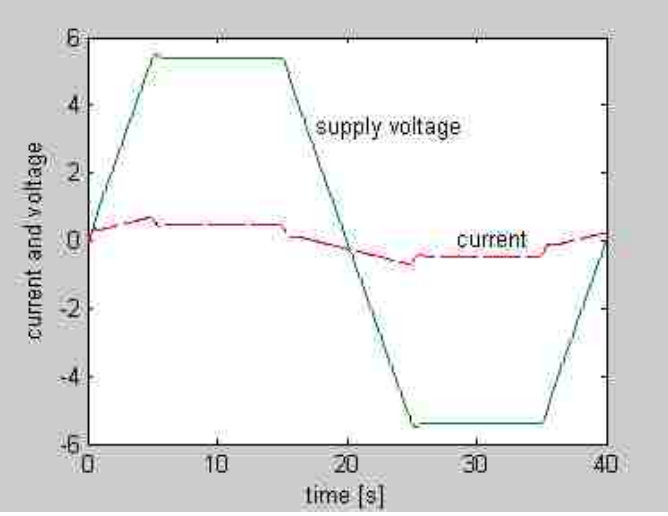

Figure 7.2.a Current and voltage waveforms of four-quadrant operation of DC motor

7.3 Four-Quadrant Operation of DC Motor in Real-Time

In real-time Simulink model the **Wref_4quad** block is used too to generate the alternating reference speed command to the DC motor through speed and current controllers (Fig. 6.3). The **Switch** block has the following properties:

- Criteria for passing first input: **u2 > Threshold**
- Threshold: **0.1**

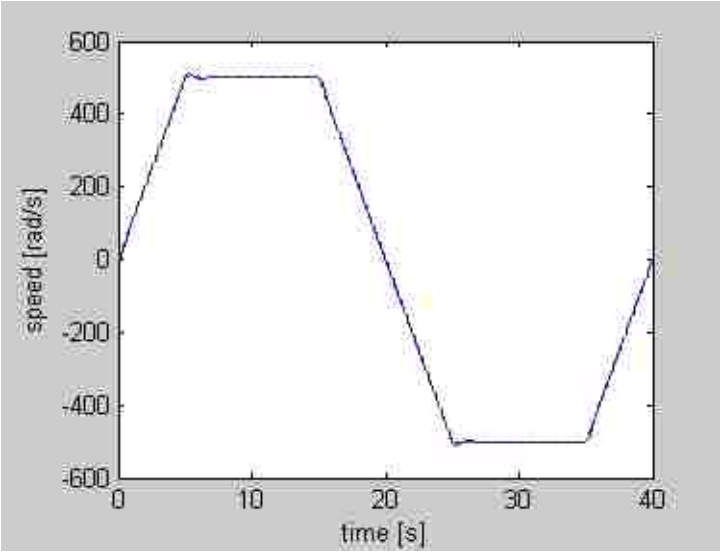

Figure 7.2.b Speed waveform of four-quadrant operation of DC motor

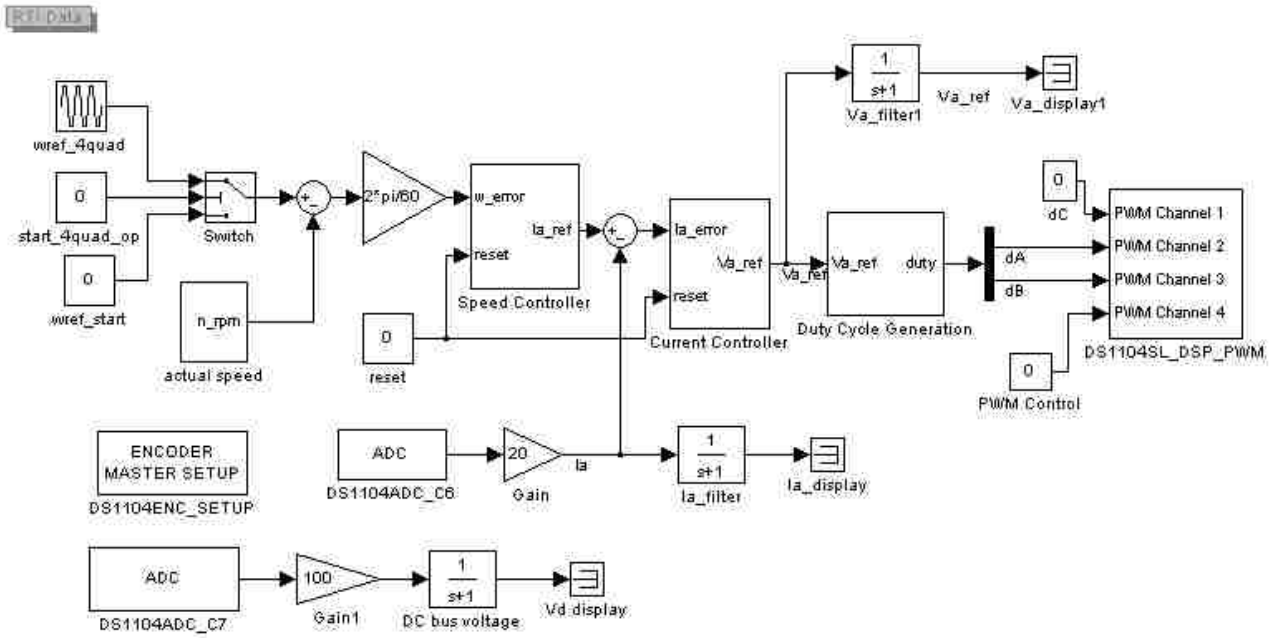

Figure 7.3 Real-time Simulink model for four-quadrant operation of DC motor

At the starting (when system is initiated to run) the value of **start_4quad_op** is **0**, so the **Switch** block takes the reference speed value from **Wref_start.** Thus, at this time the motor will rotate in

first quadrant only. The four quadrant operation is achieved when the value of **start_4quad_op** is changed to **1**.

Sub-system blocks of real-time Simulink model for four-quadrant operation of DC motor:

– Speed measurement block (actual speed) (Fig. 7.4)

The speed of the DC motor is measured using this sub-system block. A **Gain** block with a value of **60/(2*pi)** is connected to the output of averaging block (Fig. 7.4) to convert the motor speed from **rad/s** to **r/min**. The **Gain** block with the value of **(2*pi)/60** is connected (Fig. 7.3) to **Speed Controller** block in order to convert back the speed from **r/min** to **rad/s**.

Figure 7.4 Speed measurement subsystem

– Speed Controller (Fig. 7.5)

The controller gains values (Kp_w and Ki_w), determined in previous experiment (DC motor speed control), are used in this experiment. The limit value of the **Integrator** and **Saturation** blocks of the Speed Controller contains **rated current** value of the DC motor.

Figure 7.5 Speed controller subsystem

– Current Controller (Fig. 7.6)

The values of controller gains (Kp_i and Ki_i) determined in previous experiment (DC motor speed control) are used here. The limit value of the Integrator and Saturation blocks of the Speed Controller contains **rated voltage** value of the DC motor.

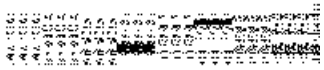

Figure 7.6 Current controller subsystem

– Duty cycle generation (Fig.7.7)

The duty cycles for **DS1104SL_DSP_PWM** block are generated by sub-system block **Duty Cycle Generation**. Its parameters were determined in the previous experiments.

Figure 7.7 Duty cycle generation subsystem

The analog input channels **DS1104ADC_C6** and **DS1104ADC_C7** in Fig. 7.3 are used to sense the motor current and DC bus voltage respectively.

The Simulink model is built in real-time and the Control Desk layout for this model is presented in Fig. 7.8. The four-quadrant operation of DC motor is achieved after checking the **start_4quadop** check box in Control Desk. By this the motor speed follows the reference speed command provided by the **wref_4quad block**.

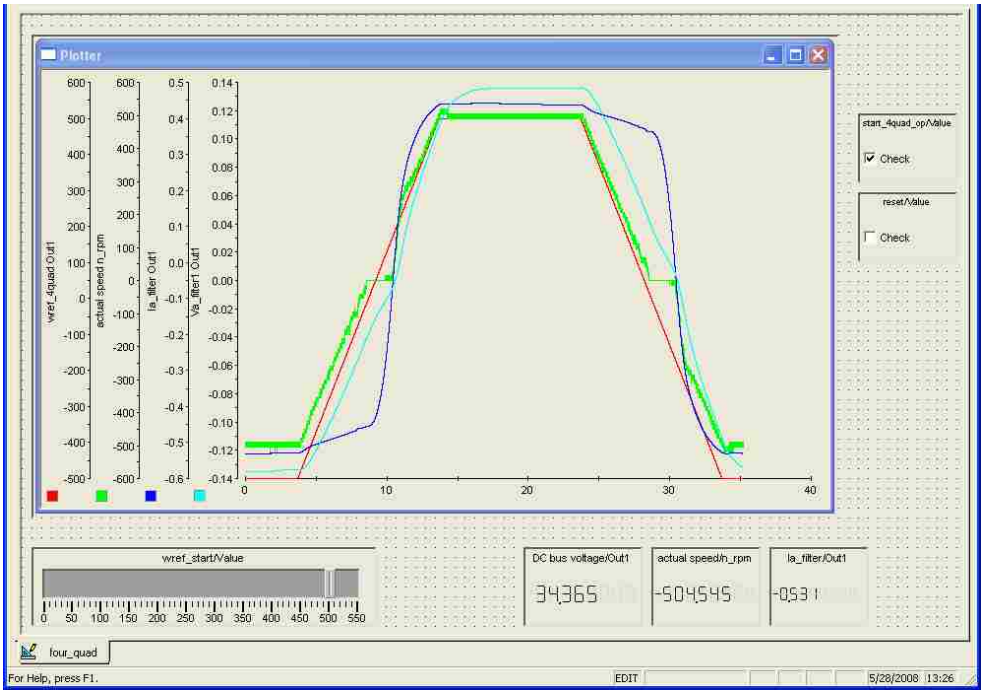

Figure 7.8 Control desk layout for four-quadrant control of DC motor

The motor operation in four quadrants is illustrated in Fig. 7.9 [7]. According to this diagram the particular mode of DC motor operation is as follows:

1) quadrant I – forward motoring:

$V_a > 0, I_a > 0 \; and \; \omega_m > 0$

2) quadrant III – reverse motoring:

$V_a < 0, I_a < 0 \; and \; \omega_m < 0$

3) quadrant II:

a) $V_a > 0, I_a < 0 \; and \; \omega_m > 0 \; forward \; regenerative \; braking$

b) $V_a < 0, I_a < 0 \; and \; \omega_m > 0 \; forward \; braking$

4) quadrant IV:

a) $V_a > 0, I_a > 0 \; and \; \omega_m < 0 \; reverse \; braking$

b) $V_a < 0, I_a > 0 \; and \; \omega_m < 0 \; reverse \; regenerative \; braking$

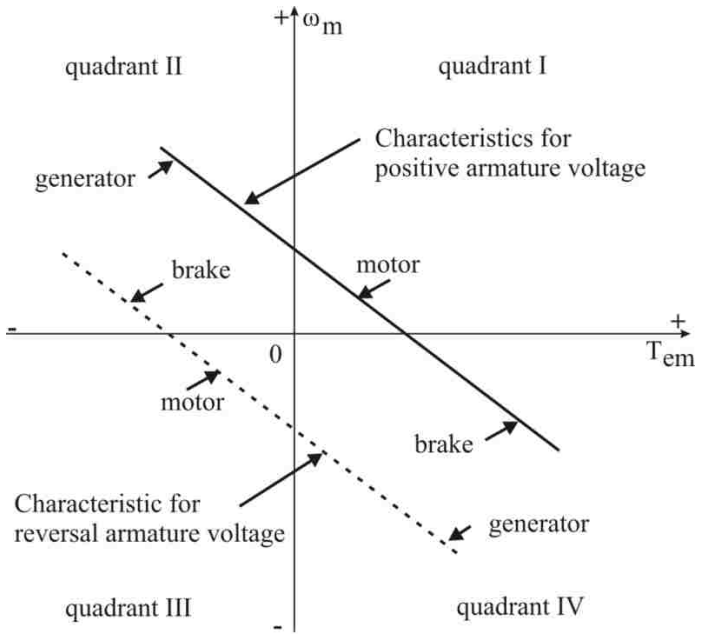

Figure 7.9 Diagram of four quadrant mode of DC motor operation [7]

The particular mode of operation region can be found in Fig. 7.10 where the graph obtained from the test is presented.

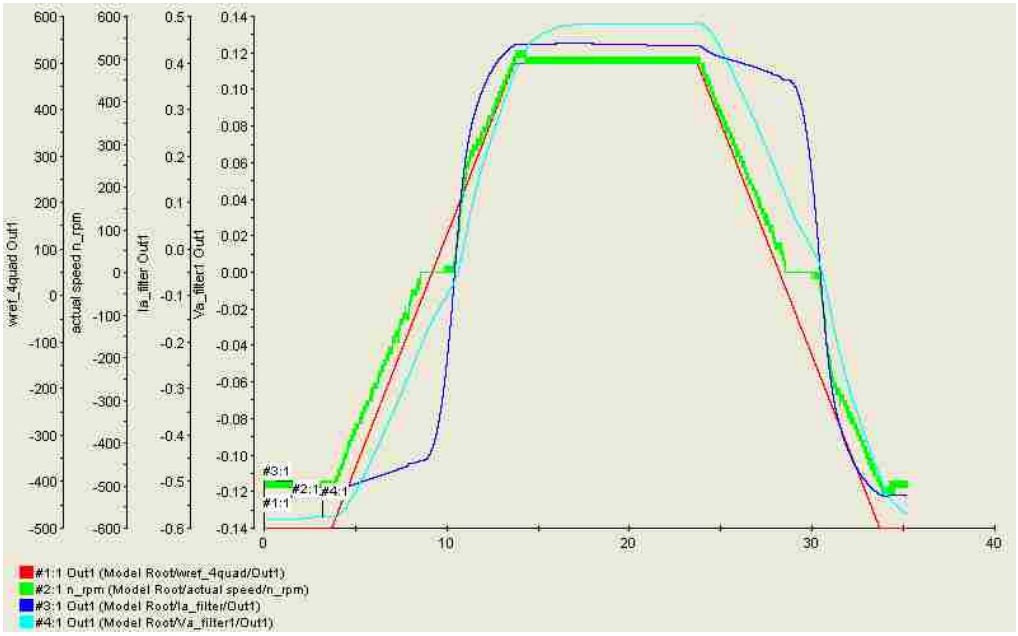

Figure 7.10 Forward and reverse motoring operation

7.4 Conclusion

In this experiment the four-quadrant operation of DC motor was examined. To do this first, the Simulink model for four-quadrant operation of DC motor was built and simulation of motor operation was performed. Next, the real-time Simulink model was built to achieve the four-quadrant operation of DC motor in real-time.

Comparing the simulation results shown in Figs. 7.2.a and 7.2.b with the measured ones no significant difference was observed. It means the Simulink motor model is an accurate tool to analyze the motor performance.

Chapter 8

Experiment 7 – Determination of Induction Motor Parameters

8.1 Introduction

In this experiment the induction motor parameters are determined using the **no-load** test and **blocked rotor** test. To perform these tests the three-phase induction motor is axially coupled with the DC motor and both are supplied from two independent PWM converters in four-quadrant configuration. The circuit diagram for the parameter determination of three-phase induction motor is shown in Fig. 8.1.

The per-phase equivalent circuit of the three-phase induction motor is shown in Fig. 8.2. The magnetizing reactance $\boldsymbol{X_m}$ can be determined using the no-load test. In this test the induction motor is rotated with **synchronous** speed by supplying the stator terminals with **rated voltage** and **rated frequency**. The stator leakage inductance X_{ls} and rotor circuit parameters referred to primary: $\boldsymbol{X_{lr}}$ and $\boldsymbol{R_r}$ are determined using the **blocked rotor** test. In this test the speed $\boldsymbol{\omega_m}$ is **0** and the stator is supplied with **slip frequency**.

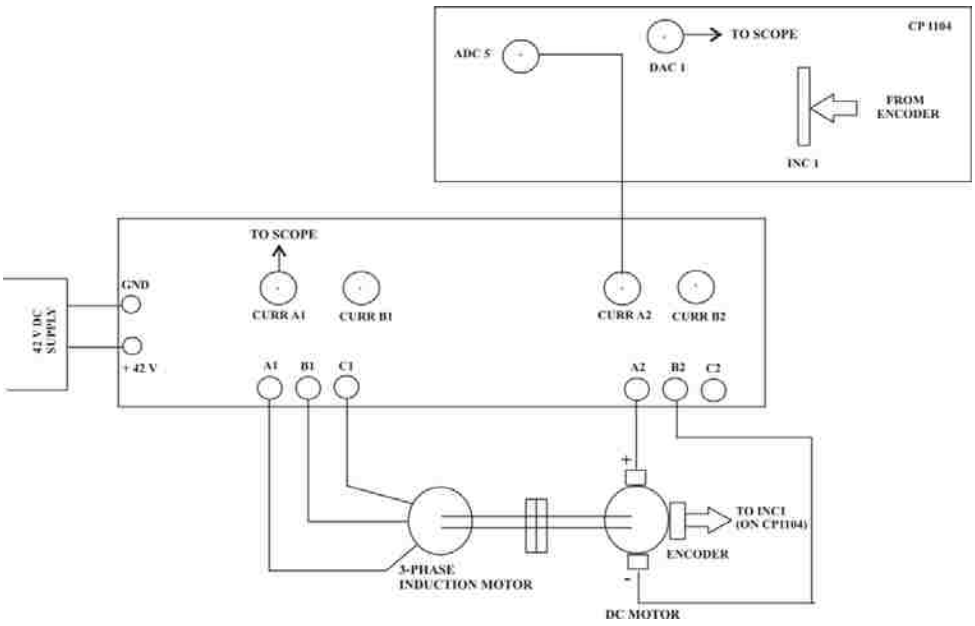

Figure 8.1 Circuit diagram for the characterization of a three phase induction motor

8.2 Theoretical Background

The induction motor is basically a transformer, whose secondary rotates with respect to the primary. The stator windings produce a rotating flux that crosses the air-gap and cuts the rotor conductors.

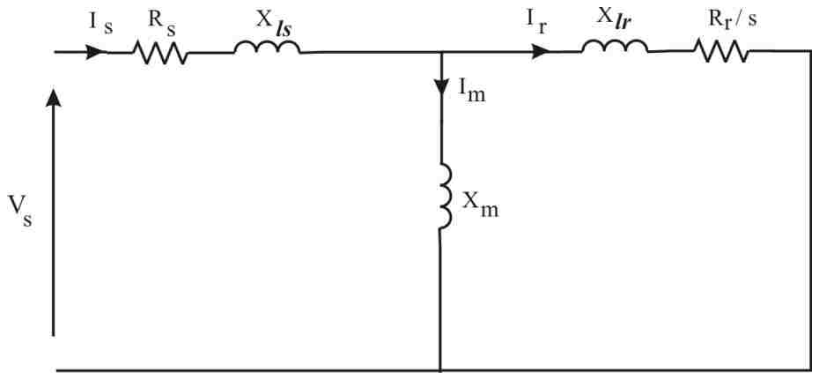

Figure 8.2 Per-phase equivalent circuit of three-phase induction motor

– Tests to determine equivalent circuit parameters

As the circuit model of induction motor is similar to that of a transformer, its parameters can be determined by means of:

- DC resistance method,
- No-load test (open circuit test in transformers),
- Blocked-rotor test (short circuit test in transformers).

– No-load test

The magnetizing inductance ($\boldsymbol{X_m = 2\pi f_s L_m}$) is determined using the no-load test. To run this test the induction motor is driven at **synchronous speed** by a **DC motor**. The equivalent circuit of single phase induction motor at synchronous speed is shown in Fig.8.3. This speed is kept constant with the help of the cascade control loop (current and speed controllers) applied to DC motor coupled with induction motor. The stator of induction motor is then energized by

applying the rated voltage at rated frequency. The slip is **0** so the rotor circuit is open (see Fig. 8.3). The rms value of voltage (V_{NL}), current (I_{NL}), and the power factor of the circuit shown in Fig. 8.3 at synchronous speed are measured using oscilloscope.

The magnetizing inductance L_m can be calculated from the equation:

$$L_m = \frac{X_m}{2\pi f_s} \tag{8.1}$$

The reactance X_m can be found from the reactive power Q_{NL}. The reactive power is consumed only by the magnetizing reactance X_m (assuming that the stator leakage reactance X_{ls} is negligible). Thus:

$$X_m = \frac{Q_{NL}}{{I_{NL}}^2} \tag{8.2}$$

where per-phase reactive power is:

$$Q_{NL} = V_{NL} \cdot I_{NL} \cdot \sin\theta \tag{8.3}$$

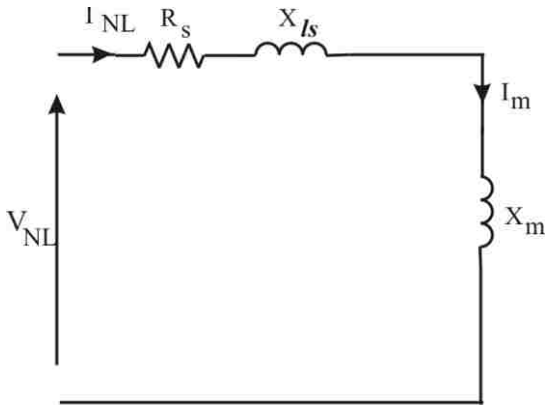

Figure 8.3 Per-phase equivalent circuit at synchronous speed (s = 0)

– Blocked rotor test

The stator leakage reactance ($\boldsymbol{X_{ls}}$), the rotor leakage reactance ($\boldsymbol{X_{lr}}$)**,** and rotor resistance ($\boldsymbol{R_r}$) are determined using blocked rotor test. To perform this test the slip frequency ($f_r = sf_s$) is

injected into the stator terminals and the rotor of induction motor is blocked such, that speed $n = 0$. The equivalent circuit model for blocked rotor test is shown in Fig. 8.4.

The value of slip is **1** when the rotor speed $n = 0$. So, the rotor circuit resistance $\left(\frac{R_r}{s}\right)$ is minimum. The rms value of voltage (V_{BR}), current (I_{BR}), and the power factor of the circuit shown in Fig. 8.4 at zero speed are measured using oscilloscope. The blocked rotor (BR) parameters can be calculated as follows [8]:

– impedance

$$Z_{BR} = \frac{V_{BR}}{I_{BR}} \tag{8.4}$$

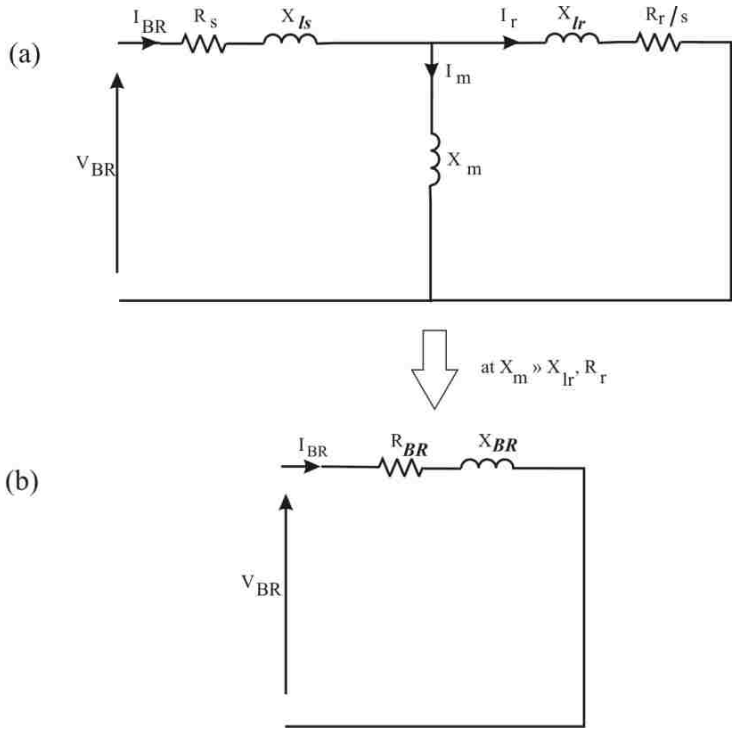

Figure 8.4 Equivalent circuit of induction motor: (a) – for rated condition, (b) – for blocked rotor test

– active power

$$P_{BR} = V_{BR} \cdot I_{BR} \cdot \cos\theta \tag{8.5}$$

– equivalent resistance

$$R_{BR} = \frac{P_{BR}}{{I_{BR}}^2} \tag{8.6}$$

where:

$$R_{BR} \cong R_s + R_r \tag{8.7}$$

– equivalent reactance

$$X_{BR} = \sqrt{{Z_{BR}}^2 - {R_{BR}}^2} \tag{8.8}$$

where:

$$X_{BR} \cong X_{ls} + X_{lr} \tag{8.9}$$

From Eqn.8.7 we have

$$R_r \cong R_{BR} - R_s \tag{8.10}$$

The particular reactance can be found from the assumption:

$$X_{ls} = \frac{2}{3} X_{lr} \tag{8.11}$$

8.3 Simulink Model and Real-Time Implementation

The real-time Simulink model for determining the parameters of three-phase induction motor is shown in Fig. 8.5. The parameters for the induction motor (IM) block set are as follows:

– Duty Cycle Generation IM (Fig. 8.6):

The duty ratios d_A, d_B, d_C of **DS1104SL_DSP_PWM3** block in Fig. 8.5 is supplied from **Duty Cycle Generation IM** sub-system block. This sub-system block uses the Eqns. 8.12

through 8.14 to provide three-phase balanced voltage with variable magnitude and frequency in order to run the induction motor at synchronous and slip speed [4]:

$$d_A = u[1] * \cos([u2]) + 0.5 \tag{8.12}$$

$$d_B = u[1] * \cos([u2] - 2 * pi/3) + 0.5 \tag{8.13}$$

$$d_C = u[1] * \cos([u2] - 4 * pi/3) + 0.5 \tag{8.14}$$

where:

$$u[1] = \frac{V_m}{V_d}$$

$$u[2] = 2\pi ft = 2\pi f \frac{1}{s}$$

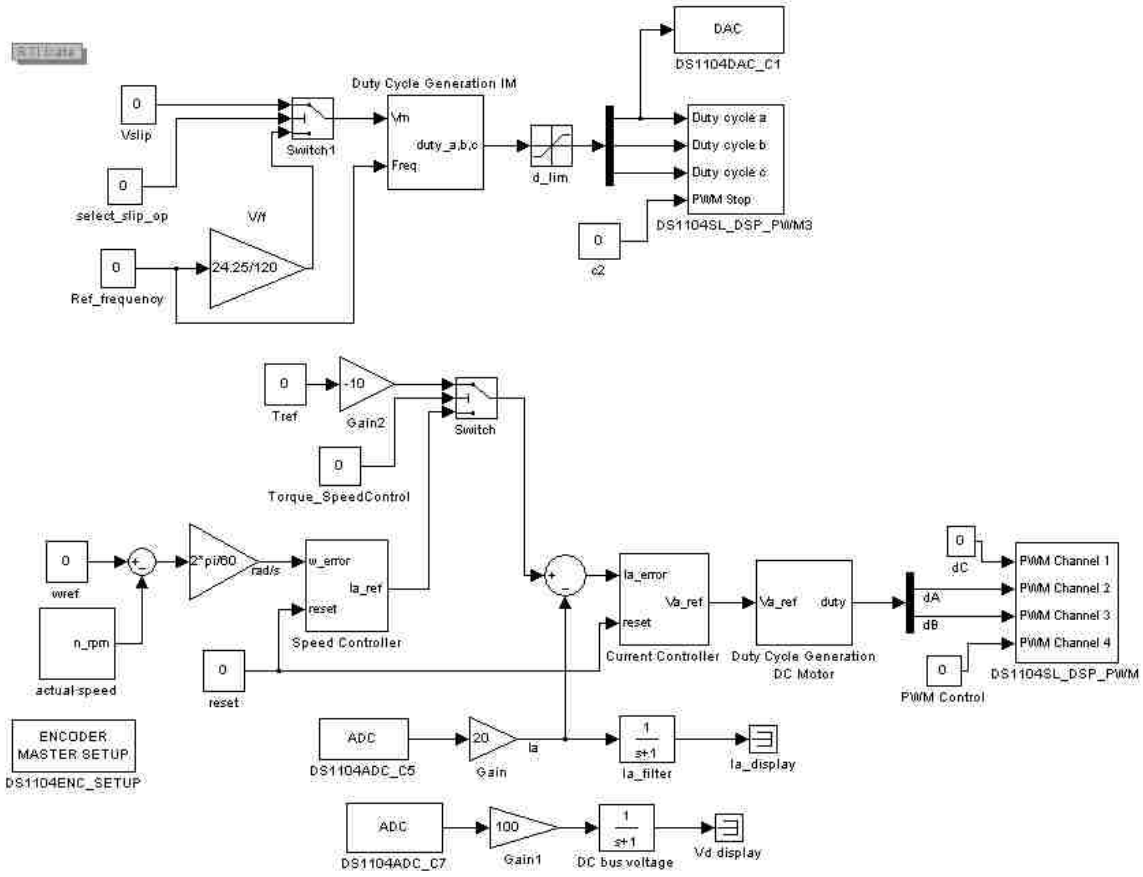

Figure 8.5 Simulink model for characterization of induction motor

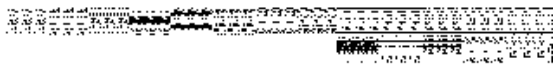

Figure 8.6 Duty cycle generation of three-phase induction motor

Constant blocks in Simulink model (Fig. 8.5)

- **Vslip:** It is used when performing the blocked-rotor test.
- **select_slip_op:** This block is used to provide the reference for the magnitude of three-phase voltage either from **Vslip** or from gain **V/f** block. The gain V/f block generates the magnitude proportional to the required frequency of the three phase voltage, which is applied to the induction motor.
- **Ref_frequency:** This block generates the desired frequency of the three-phase voltage.
- **Tref:** This block is used to load the induction motor by increasing the electromagnetic torque of DC motor.

The remaining blocks that are shown in Fig. 8.5 and which belong to DC motor have the same parameters as in Exp 6.

The control desk layout for the real-time Simulink model is presented in Fig. 8.7.

8.4 Determination of Induction Motor Parameters

– Determination of R_s:

The line to line resistance R_{sL} of three-phase induction motor under test is measured with the help of multi-meter and its value is: 0.52 Ω

The stator phase resistance is calculated as:

$$R_s = \frac{R_{sL}}{2} = \mathbf{0.26\ \Omega}$$

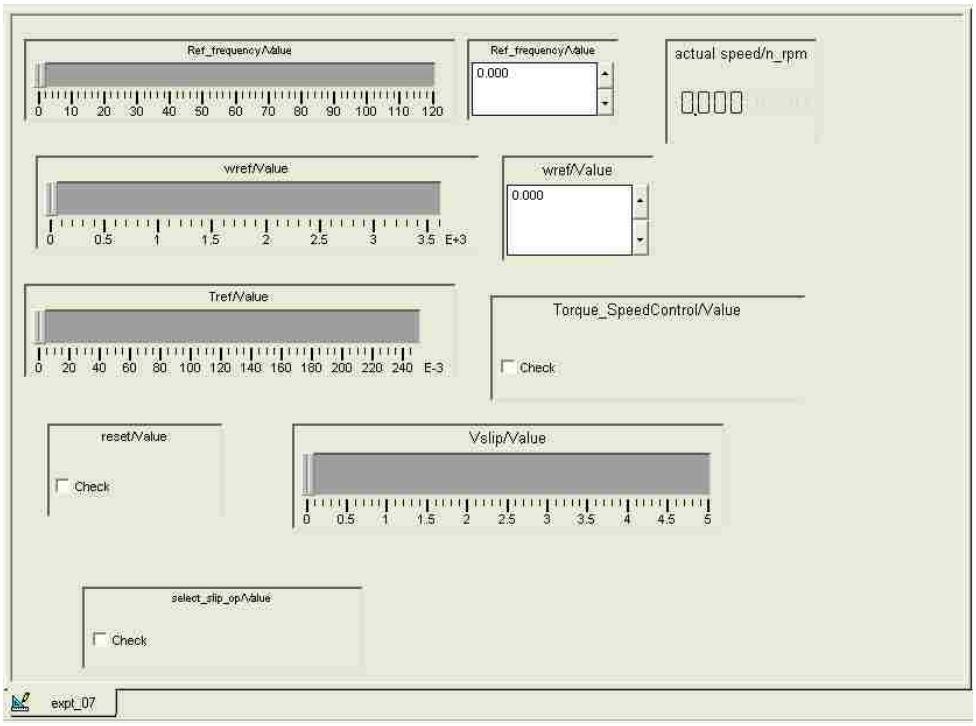

Figure 8.7 Control desk layout for motor parameters determination

– Determination of magnetizing inductance ($\mathbf{X_m = 2\pi f_s L_m}$) (no-load test)

The three-phase induction motor is rotated by DC motor at synchronous speed ($n_s = 3600\ r/min$) and is supplied with the **rated voltage** $\left(\boldsymbol{V_{L_L} = 24.25\ V}\right)$ and **rated frequency** $(\boldsymbol{f_s = 120\ Hz})$. At these operating conditions the rotor behaves as an open circuit transformer since the slip is **0**. The rms phase 'A' voltage (V_{NL}) and current (I_{NL}) are recorded and presented in Fig. 8.8. The phase difference between the two waveforms is measured to determine the power factor of the three-phase induction motor.

The phase rms voltage current and phase angle values measured on scope are given as:

$$v_{NL(measured\ on\ scope)} = 3.8\ V$$

$$i_{NL(measured\ on\ scope)} = 1.123\ A$$

$$\theta = 65^0$$

The rms voltage and current are calculated as follows:

$$V_{NL} = \frac{v_{NL,rms(measured\ on\ scope)}}{10} \times 42 \tag{8.15}$$

$$I_{NL} = i_{NL,rms(measured\ on\ scope)} \times 2 \tag{8.16}$$

where 10 and 2 are scaling factors.

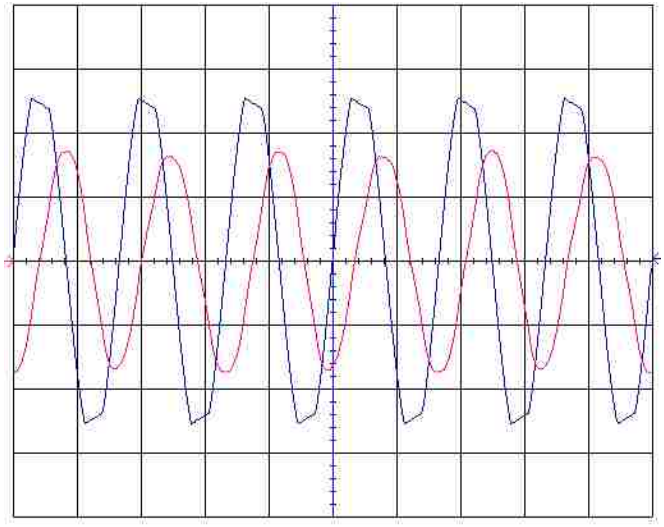

Figure 8.8 Voltage and current waveforms at synchronous speed

The per-phase reactive power is:

$$Q_{NL} = V_{NL} \times I_{NL} \times \sin\theta = 32.48\ VAR$$

where:

$$\cos\theta = power\ factor$$

This reactive power is consumed only by the magnetizing inductance since the stator inductance X_{lr} is negligible. It means that the reactive power:

$$Q_{NL} = {I_{NL}}^2 \cdot X_m \tag{8.17}$$

Thus:

$$X_m = \frac{Q_{NL}}{{I_{NL}}^2} \tag{8.18}$$

and

$$L_m = \frac{X_m}{2\pi f_s} \tag{8.19}$$

where $f_s = 120\ Hz$

By solving the above equations:

$$\boldsymbol{X_m = 6.48\ \Omega} \text{ and } \boldsymbol{L_m = 8.6\ mH}$$

– Determination of slip frequency:

The induction motor under test is loaded by the electromagnetic torque of the DC motor at the rated frequency. The induction motor is loaded until the phase current reaches the rated value (in our case 4.6 A). The speed recorded at these operating conditions: $\boldsymbol{n = 3405\ r/min.}$ The slip of the induction motor is calculated as:

$$n_{slip} = n_s - n \tag{8.20}$$

$$f_{slip} = \frac{n_{slip} \cdot p}{120} \tag{8.21}$$

where $p = number\ of\ poles$

The slip speed and frequency for $p = 4$ are:

$$\boldsymbol{n_{slip} = 195\ r/min} \ \textit{and}\ \boldsymbol{f_{slip} = 6.5\ Hz}$$

– Determination of rotor circuit parameters ($\mathbf{R_r}$, $\mathbf{X_{lr}}$) (blocked rotor test):

The stator of the induction motor is supplied with the slip frequency (f_{slip}) and the rotor is blocked. The speed of the induction motor $\boldsymbol{n}$ is **0** and the value of slip is **1**. At these operating conditions the waveforms of blocked rotor (BR) voltage (V_{BR}) and current (I_{BR}) are recorded

using the oscilloscope and the phase angle is calculated. The recorded waveforms are presented in Fig. 8.9. The actual values after multiplying measured values by the scaling factors are:

$$V_{BR} = 1.49\ V$$

$$I_{BR} = 2.28\ A$$

$$\theta = 17^{\circ}$$

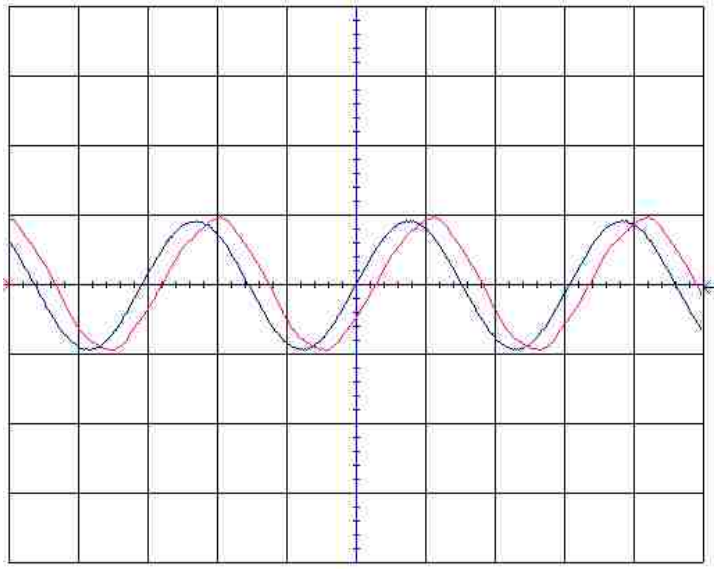

Figure 8.9 Voltage and current waveforms of blocked rotor test

The parameters determined at the blocked rotor test are (calculated as mentioned in section 8.2):

$$\boldsymbol{R_r = 0.36\ \Omega}$$

$$\boldsymbol{X_{lr} = 0.109\ \Omega}$$

$$\boldsymbol{X_{ls} = 0.07\ \Omega}$$

8.5 Conclusion

In this experiment the three-phase induction motor parameters were determined using the no-load and blocked rotor test. In no-load test the magnetizing reactance (X_m) was determined by driving the motor at synchronous speed and supplying with rated voltage and frequency. The

stator resistance (R_s) was determined using the DC resistance method. The rotor circuit parameters were determined using the blocked rotor test. In blocked rotor test the induction motor was supplied with the slip frequency and the rotor is blocked.

The determined motor parameters are:

$$R_s = 0.26\ \Omega,\ \ X_m = 6.48\ \Omega,\ \ R_r = 0.36\ \Omega,\ \ X_{lr} = 0.109\ \Omega,\ \ X_{ls} = 0.07\ \Omega.$$

Chapter 9

Experiment 8 – V/f Speed-Control of Three-Phase Induction Motor

9.1 Introduction

In a three-phase induction motor, the synchronous speed (n_{syn}), slip speed (n_{slip}), and rotor speed (n_{m_ref}) are related by the equation [9]:

$$n_{syn} = n_{m_ref} + n_{slip} \tag{9.1}$$

where:

$$n_{syn} = \frac{120 \cdot f_{ref}}{p} \;\; and \;\; n_{slip} = \frac{120 \cdot f_{slip}}{p} \tag{9.1a}$$

$$p = number\ of\ poles$$

After substituting for n_{syn} and n_{slip} in Eqn. 9.1 we obtain:

$$f_{ref} = \frac{p}{120} \times n_{m_ref} + f_{slip} \tag{9.2}$$

The slip frequency (f_{slip}) in Eqn. 9.2 is a load dependent quantity and it can be calculated in the real-time if the load torque and the slope of the torque-speed characteristic are known. In order to produce the rated torque at the rated current a proportional amount of magnitude of three-phase voltage is applied to the motor. In V/f speed-control the constant:

$$k = \frac{V_{rated}}{f_{rated}} \tag{9.3}$$

is known as V/f constant. In section 9.3 the torque-speed characteristics for different input frequencies for variable load are determined. The slope **m** of torque-speed characteristic is calculated in section 8.4 to implement the V/f speed control.

9.2 Real-Time Implementation of V/f Speed-Control of Three-Phase Induction Motor

The real-time Simulink model for speed-control of three-phase induction motor is shown in Fig. 9.1. In this model:

- The **f_ref** block is used to determine the torque-speed characteristics of the three-phase induction motor.
- The **n_ref_r_min** is used to implement V/f speed-control of induction motor.

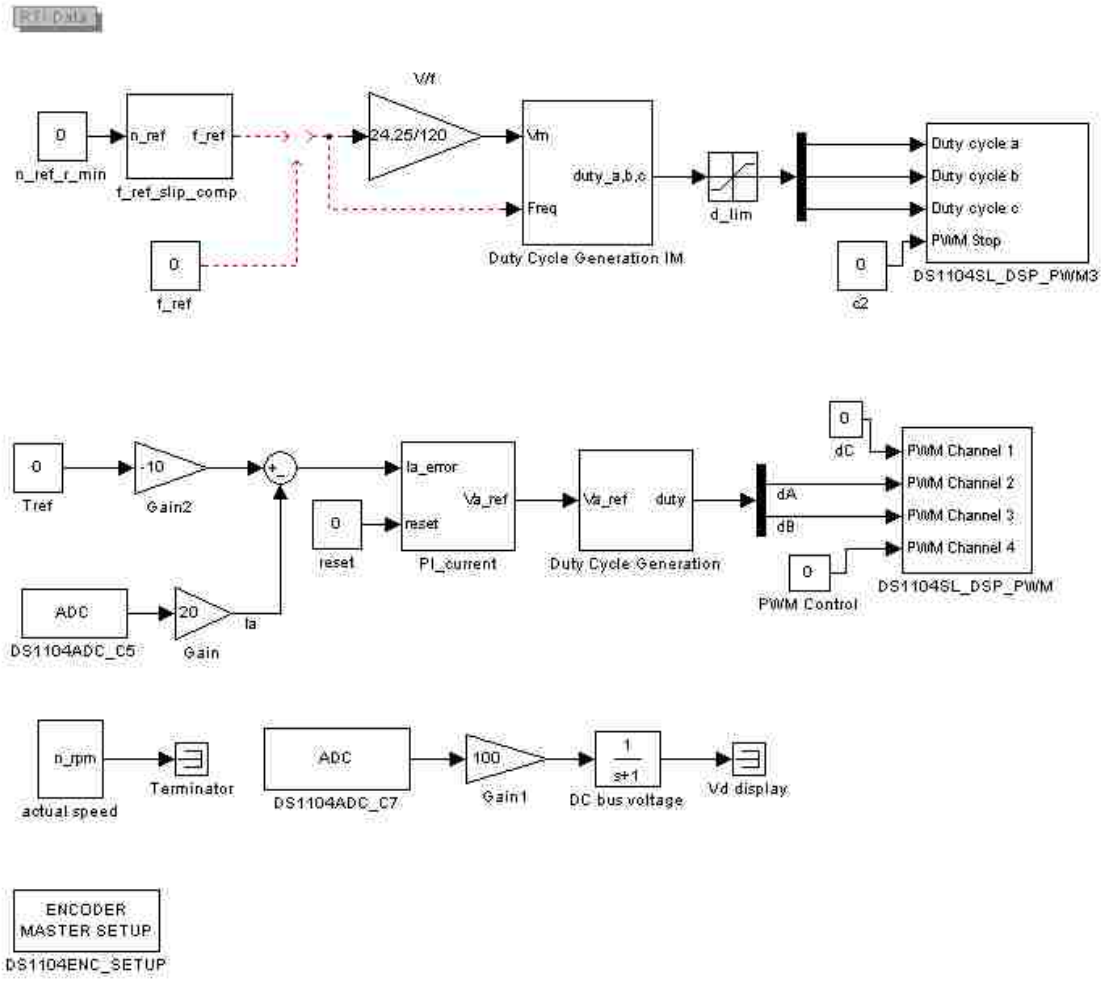

Figure 9.1 Real-time Simulink model for V/f speed-control of induction motor

- The **f_ref_slip_comp** sub-system block is used to determine the f_{ref} for a desired speed reference (**Wref_r_min**) by calculating f_{slip}. The Simulink model of the sub-system block **f_ref_slip_comp** is shown in Fig. 9.2.

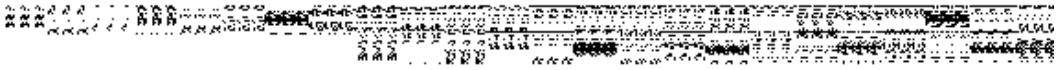

Figure 9.2 Simulink model of f_ref_slip_comp sub-system block

The Control desk layout for the Simulink model is shown in Fig.9.3.

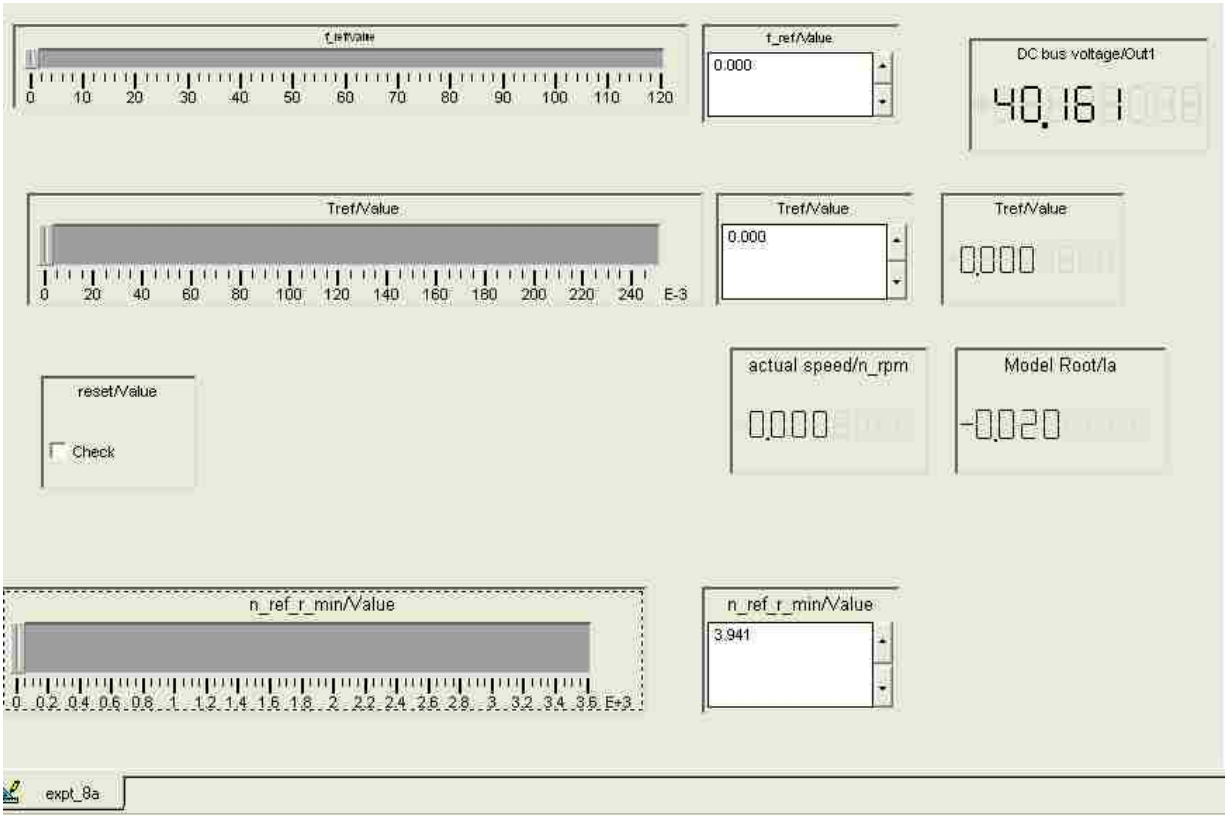

Figure 9.3 Control desk layout for V/f speed control of induction motor

9.3 Determination of Torque-Speed Characteristics

In the Simulink model (Fig.9.1) the frequency input to the **Duty Cycle Generation IM** sub-system block is from **f_ref block**. The DC motor coupled with the induction motor (Fig. 9.4) will act as a variable load and the value of the load torque is varied using the **Tref** block in Control desk. The torque T_{IM} developed by the induction motor in steady-state is equal to:

$$T_{IM} = T_{DC} + T_{fr} + B \cdot \omega \tag{9.4}$$

where:

$T_{DC} - the\ DC\ motor\ load\ torque$

$T_{fr} = 0.0362\ \ N \cdot m - constant\ friction\ torque$

$B = 0.0001 - friction\ coefficient\ of\ variable\ frictional\ torque$

The T_{fr} and B are calculated in Experiment 4 (Determination of DC Motor Parameters).

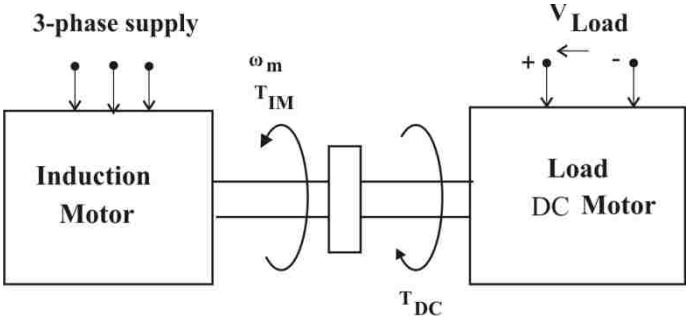

Figure 9.4 Machine set model

With the help of dSPACE board the induction motor characteristics are measured and the readings are presented in Table 9.1. The synchronous speed n_{syn} is calculated from Eqn. 9.1a, at which the induction motor torque $T_{IM} = 0$. The measurements were done for the following frequencies applied to the induction motor: [30 40 60 80 100] Hz. The characteristics are plotted in Fig. 9.5.

Table 9.1 Torque-speed characteristics for different supply frequency

f_ref [Hz]	$T_{ref} = T_{DC}$ [N·m]	n_m [r/min]	$\omega_m = (\frac{2\pi n_m}{60})$ [rad/s]	$T_{IM} = T_{DC} + T_{fr} + B \cdot \omega_m$ [N·m]
30	0	$n_{syn} = 900$	$\omega_{syn} = 94.25$	0
	0	886	92.7	0.0454
	0.025	872	91.3	0.0709
	0.050	845	88.4	0.0956
	0.075	831	87.0	0.1205
	0.100	804	84.1	0.1452
	0.125	777	81.3	0.1701
	0.150	736	77.0	0.1945
40	0	n_{syn} =1200	$\omega_{syn} = 125.6$	0
	0	1172	122.7	0.0484
	0.025	1159	121.3	0.0733
	0.050	1145	119.9	0.0981
	0.075	1138	119.1	0.1231
	0.100	1104	115.6	0.1477
	0.125	1090	114.1	0.1726
	0.150	1063	111.3	0.1973
60	0	$n_{syn} = 1800$	$\omega_{syn} = 188.4$	0
	0	1800	188.5	0.0550
	0.025	1772	185.5	0.0797
	0.050	1759	184.2	0.1046
	0.075	1745	182.7	0.1294
	0.100	1718	179.9	0.1541
	0.125	1690	176.9	0.1788
	0.150	1677	175.6	0.2037
80	0	$n_{syn} = 2400$	$\omega_{syn} = 251.3$	0
	0	2386	250.0	0.0618
	0.025	2372	248.5	0.0866
	0.050	2359	247.0	0.1115
	0.075	2331	244.1	0.1356
	0.100	2304	241.2	0.1603
	0.125	2290	239.8	0.1851
	0.150	2277	238.4	0.2100
100	0	$n_{syn} = 3000$	$\omega_{syn} = 314.1$	0
	0	2972	311.2	0.0673
	0.025	2959	309.8	0.0921
	0.050	2945	308.3	0.1176
	0.075	2931	306.9	0.1418
	0.100	2904	304.1	0.1666
	0.125	2890	302.6	0.1914
	0.150	2877	301.2	0.2163

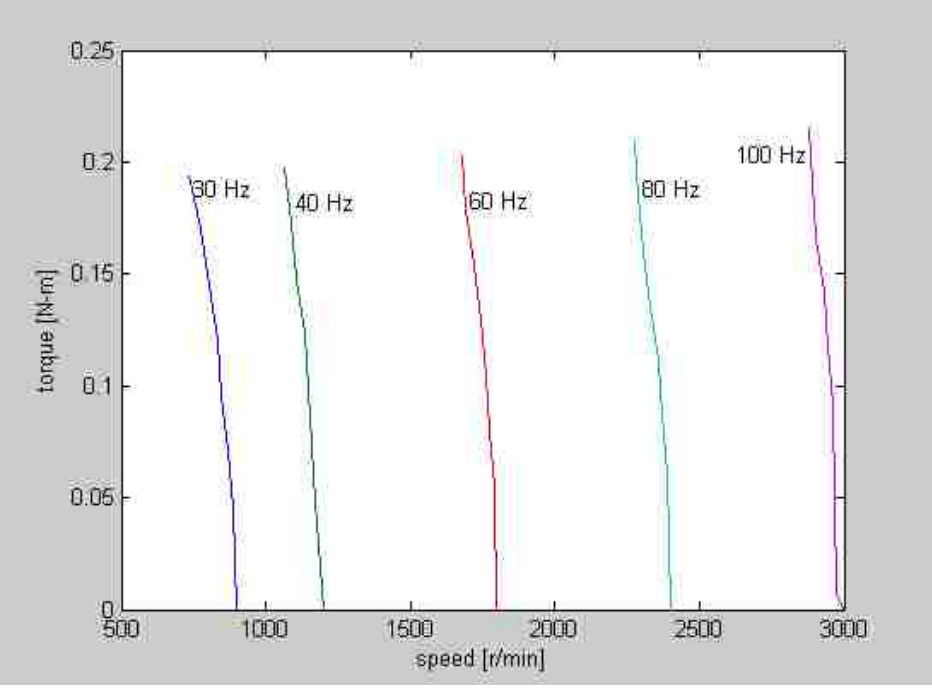

Figure 9.5 Torque-speed characteristics for different f_ref

They can be approximated by the equation:

$$T_{IM} = m \cdot n_m + c$$

where:

$n_m = the\ rotor\ speed\ in\ rpm$

$m = slope\ of\ the\ characteristic\ in\ Fig.\ 9.5$

$c = intercept\ of\ the\ characteristic\ in\ Fig.\ 9.5$

For each of this characteristics m_i and c_i are calculated and the results are presented in Table 9.2. Then the average value of m and c is calculated as:

$$m = \frac{\sum_{i=1}^{n} m_i}{n}, \qquad c = \frac{\sum_{i=1}^{n} c_i}{n} \tag{8.5}$$

where n = 5.

The average values of m and c are written Table 8.3

Table 9.2 Calculated parameter m and c

f_ref [Hz]	slope (m_i) [N·m/r/min]	intercept (c_i) [N·m]
30	-0.0011	1.0418
40	-0.0014	1.7318
60	-0.0014	2.6161
80	-0.0014	3.5041
100	-0.0018	5.4636

Table 9.3 Average value of slope (m) and intercept (c)

slope (m) [N·m/r/min]	intercept (c) [N·m]
-0.00142	2.87114

The slope (m) and intercept (c) for frequency f_ref = 30 Hz of the torque-speed characteristics in Fig. 9.5 are calculated in Matlab command window as:

Speed = [900 886 872 845 831 804 777 736]

Torque = [0 0.0454 0.0709 0.0956 0.1205 0.1452 0.1701 0.1945]

p = polyfit (Speed, Torque, 1)

m = p(1) = -0.0011

c = p(2) = 1.0418

From Fig.9.5 one can see that as the speed increases the torque developed by the induction motor sharply decreases. When the speed of the induction motor reaches synchronous speed the torque developed by the induction motor is 0.

9.4 Speed-Control of Three-Phase Induction Motor at Constant V/f Ratio

The machine set diagram for the speed-control of three-phase induction motor at constant V/f ratio is shown in Fig. 9.6.

The induction motor is coupled with DC motor, which does not produce any electrical torque. The load torque for the machine set at this condition is as follows:

$$T = T_{fr} + B \cdot \omega \tag{9.6}$$

Since T_{fr} and B are known from previous experiment (Expt 4), torque for a given mechanical speed can be calculated.

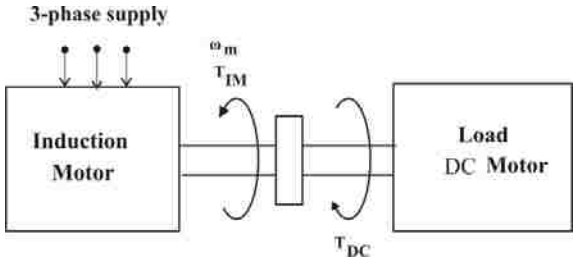

Figure 9.6 Machine set model for speed-control of induction motor

In order to rotate the induction motor with the above reference mechanical speed (see Eqn. 9.6) the reference frequency supplied to the stator terminals should be calculated using the torque-speed characteristics in the following way:

Let the mechanical reference speed in rad/s be ω_m. From the Eqn. 9.6 the torque (T_{IM}) at this speed will be:

$$T_{IM} = T_{fr} + B \cdot \omega_m \tag{9.7}$$

Also let the equation of the torque-speed characteristics be:

$$T = m \cdot n_m + c \tag{9.8}$$

where:

$m = slope\ of\ the\ characteristics\ in\ N \cdot m/(r/min)$

$c = constant$

Thus,

$$T_{fr} + B\omega_m = m \cdot n_{m_ref} + c \tag{9.9}$$

since:

$$\omega_m = \frac{2\pi n_{m_ref}}{60}$$

$$c = T_{fr} + B\omega_m - m \cdot n_{m_ref} \tag{9.10}$$

At synchronous speed $n_m = n_{syn}\ and\ T_{lM} = 0$. Then from Eqn. 9.8

$$0 = m \cdot n_{syn} + c \tag{9.11}$$

Thus, combining Eqns. 9.10 and 9.11 we obtain:

$$n_{syn} = -\frac{c}{m} = -\frac{T_{fr} + B\omega_m - m \cdot n_{m_ref}}{m} = n_{m_ref} + n_{slip} \tag{9.12}$$

From Eqn. 9.12 we obtain:

$$n_{slip} = -\frac{T_{fr} + B\omega_m}{m} \tag{9.13}$$

Having known n_{syn} from Eqn. 9.12, the frequency to be applied to the induction motor can be calculated for a 4-pole motor as:

$$f_{ref} = \frac{p \times n_{syn}}{120} = \frac{n_{syn}}{30} \tag{9.14}$$

The Eqns. 9.13 and 9.14 are used in the Simulink model to generate **f_ref** in **f_ref_slip_comp** sub-system block (see Fig. 9.1). The $\frac{1}{m}$ gain block used in this Simulink model has the value of **704,** which was calculated in the previous section (9.3).

The input frequency to the **Duty Cycle Generation IM** sub-system block of real-time Simulink model for the V/f speed-control is given from the **f_ref_slip_comp** sub-system block.

Using the dSPACE control desk the test has been carried out and the speed values measured for the different reference speed $\left(n_{m_ref}\right)$ are listed in Table 9.4.

Table 9.4 Measured speed values using the slip compensator

Reference speed n_{m_ref} [r/min]	Actual speed n_m [r/min]
500	504
1200	1213
2000	2027
3000	3036

The difference between the actual and reference speed values in Table 9.4 is due to the slip compensator gain block $\frac{1}{m}$ in **f_ref_slip_comp** sub-system block in Simulink model. For different input reference speed values the **f_ref_slip_comp** sub-system block generates the corresponding reference frequency (f_{ref}).

9.5 Conclusion

The reference frequency of the three-phase induction motor is generated by finding the slip frequency (Eqn. 9.12) using the torque-speed characteristics. These characteristics are listed in Table 9.1. The average slope value (m) determined using these characteristics is used as the slip compensator in **f_ref_slip_comp** sub-system block of the real-time Simulink model (Fig. 9.1) to obtain the speed-control of induction motor at constant V/f ratio.

Chapter 10

Conclusions and Future Scope of Study

10.1 Conclusions

The Thesis project was focused on lab experiments prepared for EE 4490 Adjustable Speed Drives course, which is taught at Louisiana State University (LSU). The outcome of the project is the Lab Manual and this thesis, which is the lab report to the experiments described in the Manual.

The Manual was prepared on the basis of DSP Based Electric Drives Laboratory User Manual, University of Minnesota.

The experiments have been modified to the needs of EE 4490 course and according to the equipment available in Electrical and Computer Engineering Department at LSU.

The Lab Experiments have been scheduled in such a way that students gradually learn modeling dynamics of electromechanical systems in Matlab/Simulink, beginning from very simple mechanical systems (Experiment 1) to more complex systems on feedback control of DC drives (Experiment 5 and 6) and open-loop V/f control of induction motors (Experiment 8). Having learned Simulink modeling students start programming the DSP controllers where Simulink drive models are used, and which allow controlling the real electromechanical systems in real-time (Experiments 4, 5, 6, 7, 8).

The use of dSPACE controllers, which utilize the Simulink modeling in Programming, is the major advantage over other systems in real-time control.

Summarizing, the experiments prepared for Laboratory of EE 4490 course allow students to learn designing speed controllers of DC and AC drives and to control them in real-time.

10.2 Future Scope of Study

The experiments that were developed are mainly focused on control of DC electric drive. Only the last two experiments concerned the induction motor drive: One of them concentrated on determining the motor characteristics, the other one was on open-loop V/f speed control of induction motor.

With the available lab equipment additional lab experiments on AC drives can be developed. Namely:

- Close-loop vector control of induction motor
- Open-loop speed control of PM synchronous motor
- Close-loop speed control of PM synchronous motor (brushless DC motor)
- Switched reluctance motor drives

All these experiments could enhance EE 7490: Advanced Electric Drives course taught for graduate students.

Thus, the future work should concentrate on the development of the above mentioned experiments.

References

[1] Mendrela, "DC Motor Drives" Lecture notes, Louisiana State University, Baton Rouge, LA.

[2] DSP based Electric Drives Laboratory User Manual, University of Minnesota 2004.

[3] "Restructing of First Course in Power Electronics and Electric Drives that Integrates Digital Control" IEEE *"transaction"* on Power Electronics, Vol. 18, January 2003.

[4] Ned Mohan: *Electric Drives an Integrated Approach*, MNPERE Publishers, Minnesota, 2001.

[5] Mendrela "Dynamic Simulation of an Elevator driven by DC Motor" Lecture notes, Louisiana State University, Baton Rouge, LA.

[6] Stephen J. Chapman: *Electric Machinery Fundamentals, Fourth Edition*, McGraw-Hill, 2004.

[7] Mendrela "Introduction to DC Motors" Lecture notes, Louisiana State University, Baton Rouge, LA.

[8] D.P. Kothari and I.J. Nagrath: *Electric Machines, Third Edition,* McGraw-Hill, 2004.

[9] DSP based Electric Drives Laboratory User Manual, University of Minnesota 2007.

[10] Ned Mohan: *Advanced Electric Drives* MNPERE Publishers, Minnesota, 2001.

[11] M.Gopal: *Control Systems: Principles and design*, McGraw-Hill, 2002.

[12] Allen R. Stubberud: *Feedback and Control Systems, Second Edition*, McGraw-Hill.

[13] Irveng L. Kosow: *Electric Machinery and Transformers, Second Edition*, Prentice Hall.

[14] Mohammed A. El-Sharkawi: *Fundamentals of Electric Drives First Edition,* Thomas Learning

[15] R. Krishnan: *Electric Motor Drives, Modeling Analysis, and Control,* Prentice Hall, 2001.

[16] Hamid A. Toliyot: *DSP-Based Electromechanical Motion Control,* CRC Press, 2004.

Vita

Kiran Kumar Gunda, son of Laxmikantham Gunda and Padmavathi Gunda, was born in Godavarikhani, India. He completed his schooling in Vani Vidya Vihar High School, Godavarikhani. He pursued his Bachelor of Technology in Electrical and Electronics Engineering in distinction from Jawaharlal Nehru Technological University in 2005. He joined the Department of Electrical and Computer Engineering at Louisiana State University in August 2006 to pursue his master's degree. He will be awarded the degree of Master of Science in Electrical Engineering in August 2008.